Scandinavia

John A. Matthews and Atle Nesje

1 Introduction

For purposes of this chapter, Scandinavia is defined as four countries—Norway, Sweden, Finland and Denmark—which occupy a total area of ~1.2 million km^2, which is over one tenth of the area of Europe. By virtue of their northerly location, latitudinal extent and topography, the present-day periglacial landscapes of Scandinavia exhibit characteristics of both Arctic and alpine regions (Fig. 1). Most of these periglacial landscapes are located in the 'Scandes', the Scandinavian mountain chain that extends from southern Norway to northern Finland. The Scandes occupy more than one-third of the area of Norway, almost one-tenth of the area of Sweden and a very small part of northern Finland (Corner 2005a). They rise to 2469 m above sea level in Jotunheimen, southern Norway, and 2097 m a.s.l. in Kebnekaise, northern Sweden, and include extensive plateau areas that lie generally between 1000 and 1500 m a.s.l. Together with high-level basins, valleys and cols, the plateaux have been seen as macro-remnants of 'palaeic' landscapes, which retain pre-Pleistocene characteristics little modified by subsequent uplift and glaciation (Holtedahl 1960; Gjessing 1967; Lidmar-Bergström et al. 2000). According to Etzelmüller et al. (2007) such 'palaeic' landscapes may account for ~12% of the surface area of southern Norway.

J. A. Matthews (✉)
Department of Geography, College of Science, Swansea University, Singleton Park, Wales SA2 8PP, UK
e-mail: J.A.Matthews@Swansea.ac.uk

A. Nesje
Department of Earth Science and Bjerknes Centre for Climatic Research, University of Bergen, NO-5020 Bergen, Norway
e-mail: Atle.Nesje@uib.no

M. Oliva et al. (eds.), *Periglacial Landscapes of Europe*,
https://doi.org/10.1007/978-3-031-14895-8_14

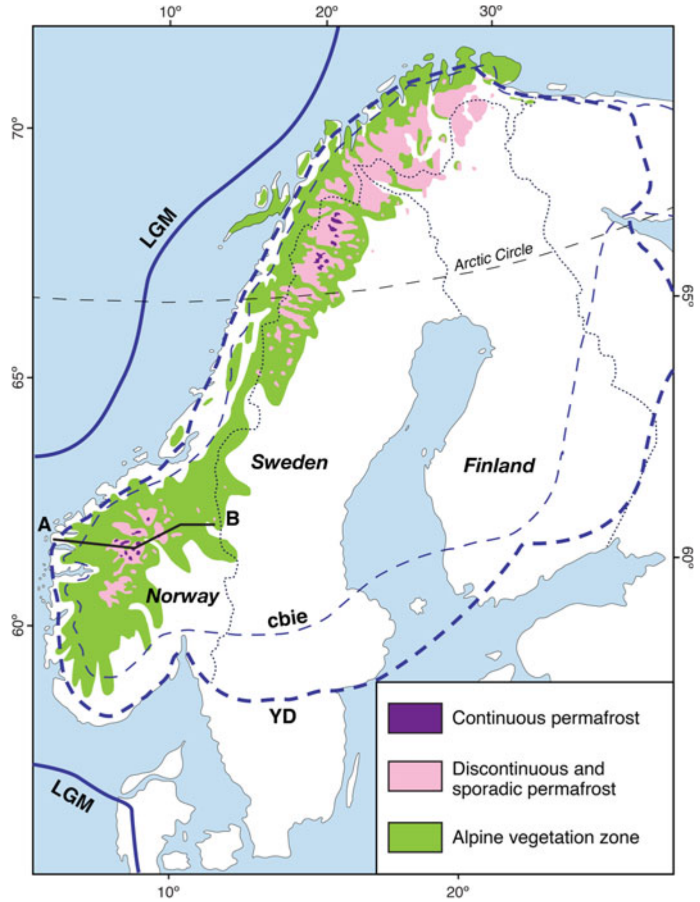

Fig. 1 Geographical background to Scandinavian periglacial landscapes: permafrost zonation (generalised from Gisnås et al. 2017); the alpine vegetation zone (based on Moen 1999; Heikkinen 2005), which approximates the zone of geomorphologically significant seasonal frost; limits of the Scandinavian Ice Sheet at the Last Glacial Maximum (LGM, 22–21 ka) and during the Younger Dryas (YD, ~12.7 ka), and the minimum cold-based ice extent (cbie) at the Last Glacial Maximum (all based on Strøeven et al. 2016). Continuous permafrost occupies 90–100% of the present landscape within the purple area; discontinuous and sporadic permafrost >10% within the pink area. Line (A–B) defines the topographic profile shown in Fig. 2

1.1 Geological, Climatic and Geo-Ecological Background

The mountains and plateaux consist mainly of metasedimentary and metavolcanic lithologies (including schist, quartzite and amphibolite) in Caledonian nappes, which overly and have incorporated slices and blocks of granite and gneiss of the crystalline basement rocks (Corner 2005a). These lithologies are relatively resistant to weathering and erosion by periglacial and other Earth surface processes. Exposed bedrock and patchy, generally thin, superficial covers of periglacial and glacigenic regolith are characteristic of the mountains and plateaux. Increasing thicknesses of this regolith occur at lower elevations and on lower slopes, with the addition of fluvial and lacustrine sediments on the floors of valleys and basins.

Mean annual air temperature (MAAT) in Scandinavia varies from <–4 °C on the highest mountains of the Scandes to >6 °C in the southern lowlands and around 0 °C at sea level in the far north (Tikkanen 2005; Gisnås et al. 2017). The corresponding ranges of mean January and July temperature are <–14 °C to >0 °C, and <6 °C to >16°, respectively. These climatic data reveal a very wide range of climatic regimes from permafrost, through seasonal frost to cool temperate climates, within which latitude, altitude and continentality gradients are important controls.

Other annual and seasonal climatic parameters have important effects in Scandinavian periglacial landscapes. Prevailing westerly wind systems bring mean annual precipitation totals of >2000 mm over wide areas of the western slopes of the Scandes. Orographic effects are extreme, with precipitation totals in parts of the mountains >4000 mm, reducing to <400 mm in the corresponding rain-shadow areas of both Lapland and interior southern Norway (Tikkanen 2005). Maximum snow depth is 2–5 m in the western parts of the mountains and normally <2 m over most areas east of the watershed, including many high plateau areas (Gisnås et al. 2017). Mean annual ground surface temperature (MAGT) tends to be ~1 °C lower than the MAAT at exposed sites and the thermal offset may be up to ~4 °C at sites with prolonged snow (Farbrot et al. 2011). Local snow distribution is the result of complex interactions between temperature, precipitation, wind, radiation, and local topography (Liston and Elder 2006), and affects many periglacial processes through microclimate and hydrology.

Geoecosystems are equally varied and are also largely determined on macro- to micro-scales by climate. Above and beyond the tree line, which normally involves mountain birch (*Betula pubescens*) and, in some regions, Scots pine (*Pinus sylvestris*), the alpine zone is commonly subdivided into high-, mid- and low-alpine belts on the basis of the plant communities (Moen 1999; Heikkinen 2005). In southern Scandinavia, permafrost is largely confined to the high- and mid-alpine belts, and the tree line (lower limit of the dwarf shrub-dominated low-alpine zone) can be considered as approximating to the lower limit of effective geomorphic activity associated with seasonal frost. On the northernmost coast, the tree line descends to sea level, and in the inland continental areas to the east of the northern Scandes, the tree line corresponds approximately with the lower limit of discontinuous permafrost.

1.2 Permafrost Distribution and Limits

In the context of Europe, Scandinavia is particularly important for the extent of periglacial environments in general and permafrost in particular. The estimated total land area with permafrost in Scandinavia is ~62,600 km^2, of which 2% has been classified as continuous, 20% as discontinuous, and 78% as sporadic (Gisnås et al. 2017).

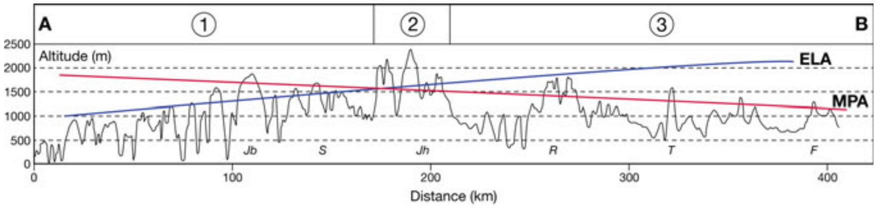

Fig. 2 A topographic profile across southern Norway defining three morphogenetic zones based on the lower altitudinal limit of (discontinuous) mountain permafrost (MPA, *red line*), and the modern glacial equilibrium-line altitude (ELA, *blue line*): (1) western zone with little or no permafrost, extensive seasonal frost and temperate glaciers (MPA > ELA); (2) central zone with extensive permafrost that co-exists in the landscape with polythermal glaciers and ice-cores moraines (MPA ≈ ELA); and (3) eastern zone where permafrost exists but glaciers are absent (ELA > MPA). The profile line (A–B), shown on Fig. 1, extends from the Norwegian west coast through the Jostedalsbreen ice-cap (Jb), Sognefjell (S), Jotunheimen (Jh), Rondane (R) and Tronfjell (T) to the Femund mountains (F) near the Swedish border (based on Etzelmüller et al. 2003; Etzelmüller and Hagen 2005)

The spatial distribution of permafrost is shown at the regional scale in Fig. 1. Altitudinal relationships are exemplified by a west-east transect across southern Norway at approximately latitude 62° N (Fig. 2) (Etzelmüller et al. 2003; Etzelmüller and Hagen 2005). This transect highlights the mountain permafrost altitude (MPA), which is equivalent to the lower altitudinal limit of discontinuous permafrost. The MPA declines from ~1750 m a.s.l. in the west to ~1350 m a.s.l. in the east, while the corresponding lower limits of sporadic permafrost occur at ~1450 m a.s.l. and ~1050 m a.s.l., respectively (Gisnås et al. 2017). Lower permafrost limits in the east reflect colder winters and decreasing snow depths associated with increasing continentality. In contrast, the equilibrium-line altitude (ELA) on the glaciers rises towards the east in response to warmer summers combined with less snow accumulation in winter.

In the Galdhøpiggen massif, Jotunheimen, in the centre of the west-east transect, several estimates place the lower altitudinal limit of discontinuous permafrost at ~1450 m a.s.l. (Ødegård et al. 1992; Isaksen et al. 2002; Farbrot et al. 2011; Lilleøren et al. 2012). There are also differences in permafrost limits between north-facing and south-facing aspects, which are most marked in relation to permafrost in steep bedrock slopes (Steiger et al. 2016; Gisnås et al. 2017). According to Hipp et al. (2014), the lower limit of discontinuous permafrost in the Galdhøpiggen massif occurs at 1500–1700 m a.s.l. in south-facing rock walls and 1200–1300 m a.s.l. in north-facing rock walls. Magnin et al. (2019) have demonstrated the occurrence of isolated, sporadic permafrost as low as 830 m a.s.l. in steep, north-facing bedrock slopes in southern Norway. However, the altitudinal limits of permafrost are not fixed. Based on borehole temperatures, Lilleøren et al. (2012) have demonstrated the scale of the altitudinal variations in permafrost limits during the Holocene. In the Galdhøpiggen massif, the lower limit of discontinuous permafrost was higher than today during the Holocene Thermal Maximum (~8.0 ka), when it was located at ~1600–1700 m a.s.l. (about 200 m higher than at present). Subsequently, a late-Holocene lowering of the limit culminated in the Little Ice Age (~AD 1750) with the aggradation of shallow permafrost possibly down to as low as ~1250 m a.s.l. (about 200 m lower than today).

In northern Scandinavia, where all permafrost limits are lower than in southern Norway, the lower limit of discontinuous permafrost decreases from ~1400 m a.s.l. in the west to generally ~400 m a.s.l. east of the Scandes (Gisnås et al. 2017). However, sporadic permafrost occurs in palsas close to sea level in northernmost Norway (Varanger peninsula) and down to ~50 m a.s.l. in Utsjoki, northernmost Finland (Seppälä 1997, 2011; Luoto and Seppälä 2002b; Miska Luoto, personal commumication). It may also occur close to sea level in steep north-facing bedrock slopes and rock glaciers (Magnin et al. 2019; Lilleoren et al. 2022). Holocene variations in permafrost limits in northern Scandinavia fluctuated within an altitudinal range of about ±100 m of today's limits (Lilleøren et al. 2012).

Permafrost thickness has been estimated as >300 m in the continuous permafrost zone at 1890 m a.s.l. in Jotunheimen, southern Norway, and at 1600 m a.s.l. in Tarfalaryggen, northern Sweden, respectively (Sollid et al. 2000; Isaksen et al. 2001; Etzelmüller et al. 2003). Active layer thicknesses of ~1.95–2.45 m have been recorded in boreholes through regolith in Jotunheimen (Harris et al 2009), ~3.0–5.0 m in rock walls in Norway (Hipp et al. 2014), and ~0.3–0.75 m in peat in northernmost Finland (Rönkkö and Seppälä 2003) where, in general, the range is ~0.5–4.0 m depending on soil type, snow depth and surface vegetation (Seppälä 2005a).

The lower regional-scale climatic limit of continuous permafrost is approximated by a MAAT of –4.0 °C, while the lower limit of sporadic permafrost can be set at –1.0 °C (King 1986; Ødegård et al. 1992; Etzelmüller and Hagen 2005). Although defining the lower climatic limit of seasonal frost is more arbitrary, a MAAT of 3.0 °C was suggested by Williams (1961) on the basis that this value is sufficient to achieve the >70 cm winter frost penetration necessary to counteract the amount of summer heat storage in the ground and to develop certain periglacial landforms (such as patterned ground and solifluction lobes). This climatic limit to the seasonal periglacial climate seems to have been widely accepted (cf. Ballantyne 2018; French 2018).

1.3 Periglacial Environments and Glacial History

Periglacial and glacial environments overlap in Scandinavia and cannot easily be separated, either as physical entities or conceptually (Etzelmüller and Hagen 2005; Berthling and Etzelmüller 2011; Miesen et al. 2021). Numerous temperate and polythermal glaciers are present in the landscape today, including the Jostedalsbreen ice cap, the largest ice body in continental Europe. During the Last (Weichselian) Glaciation, the Scandinavian Ice Sheet extended to the edge of the continental shelf and, by the end of the Late Glacial/Younger Dryas, ~11.7 ka, this ice sheet still covered most of the Scandinavian Peninsula (Hughes et al. 2016; Mangerud et al. 2016; Strøeven et al. 2016) (Fig. 1).

Throughout the Late Cenozoic Ice Age, all Scandinavian landscapes were intensely affected by numerous glacial-interglacial cycles. During the interglacials, periglacial environments were dominant. During the glacial episodes, cold-based ice sheets of varying size preserved much of the overridden landscape, while glacial erosion and deposition were most active in their marginal areas (Kleman 1994; Kleman and Hättestrand 1999; Hättestrand and Stroeven 2002; Kleman et al. 2008; Andersen et al. 2018, 2019). However, the ice sheets that occupied the Scandes for a large part of the late Pliocene and Pleistocene were smaller than those of the Last Glaciation and the other relatively recent glaciations. Such 'mountain glaciations', which are representative of 'average' glacial conditions (cf. Porter 1989), were present for an estimated 65% of the time during the last 1.88 Ma (Fredin 2002).

At the end of the Weichselian, the removal of the ice load led to uplift in response to glacio-isostatic rebound of the land mass. The land uplift was largest in the central part of Scandinavia where the relative ice thickness was largest. Uplift took place in two stages. The initial stage following deglaciation was almost immediate due to an elastic response of the crust as the ice load was reduced. Subsequently, uplift proceeded at an almost exponentially decreasing rate. The present relative land uplift rate in the northwestern part of the Gulf of Bothnia is ~9 mm/year. The total Holocene (<11.7 ka) land uplift relative to the present sea level in this area of the Gulf of Bothnia is estimated to have been ~250 m; in central southern Norway it was ~180 m; and in northern Sweden, northern Finland, and inner Finnmark, northern Norway, it was ~150 m (e.g. Vorren et al. 2006). Land uplift has shifted relative sea levels and the relative altitudinal limits of permafrost and other climate-dependant aspects of periglacial landscapes.

2 Historical Background to Research

2.1 Early Twentieth Century Beginnings

During the nineteenth century, there was little recognition of what are now known to be periglacial landforms and sediments. By the first decade of the twentieth century, however, specific landforms and sediments had been identified in Scandinavia and attributed to cold-climate processes. Lundqvist (1964) summarised influential early work from Sweden. Sernander (1905) and Andersson (1906) described different types of 'soil creep' (sorted and non-sorted patterned ground) and 'flow earth' (solifluction), while Svenonius (1909) discussed blockfield formation as being mainly formed by the disintegration of bedrock by frost, and Fries and Bergström (1910) were the first to report palsas.

A broader range of periglacial landforms was studied and theories of formation advanced during the early decades of the twentieth century. Högbom (1914, 1927), for example, classified patterned ground according to morphology, and recognised stripes, polygons, nets and circles. A Danish botanist's investigations in Greenland, carried out in the 1930s (Sørensen 1935), was important not only for his investigations into the effects of vegetation-patterned ground interaction but also for observations and measurements relating to micro-climate, soil texture, surface gradient, frost cracking, moisture-controlled density differences and 'convection currents' in the context of patterned ground, and for insights into the formation of sub-nival stone pavements involving nivation. A school of periglacial aeolian studies was established at Uppsala University in Sweden (Enquist 1916; Samuelsson 1926). At approximately the same time, coastal rock platforms in Norway were attributed to frost weathering (Vogt 1918), a process that was also seen as fundamentally important in the evolution of the Norwegian strandflat (Nansen 1922). As early as the 1930s, the effects of the freezing and thawing of sediments on roads and railways was studied in the laboratory by Beskow (1935). The English translation of his fundamental research on frost susceptibility is still widely cited (Beskow 1947).

In these early years, the development of periglacial geomorphology in Scandinavia was influenced by a number of different factors. First, Scandinavian scientists lived and worked in or near periglacial environments, which were seen as relevant. Second, explorer-scientists from Nansen (1922) to Sverdrup (1938) had taken a leading role in exploration of the Arctic, which included encounters with periglacial landscapes and active permafrost features that are not observable in Scandinavia today. Third, Scandinavian scientists were well connected with academics elsewhere in Europe and actively involved in the small but developing international periglacial research community. Following the 11th International Geological Congress held in Stockholm in 1910, the field excursion to Svalbard was particularly influential as it introduced scientists to unfamiliar permafrost environments and provided potential modern analogues for relict periglacial features elsewhere (French 2008). According to French and Karte (1988) the growth of periglacial geomorphology as an academic discipline began in 1949 with the establishment of the 'Commission on Periglacial Morphology' within the International Geographical Union. The first chairman of the Commission was the physical geographer and glaciologist, Professor H. W. Ahlmann of Stockholm University, later to become the Swedish Ambassador to Norway.

2.2 Development in the Mid- to Late-Twentieth Century

The periglacial zone had become an exemplar for climatic and climatogenic geomorphology, which developed and spread from Central Europe, especially Germany, France and Poland, during the 1940s to 1960s (André 2009). During this phase in the development of geomorphology, widespread belief in the dominance of frost action in periglacial landscapes was driven mainly by observation and mapping of landforms, combined with apparent associations with climate. Most conclusions about periglacial processes and landscape dynamics were based on inference and remained largely superficial. However, this gap in knowledge became a spur to understand better contemporary periglacial processes and climatic indicators.

André (2009) characterised the 1960s to 1980s as a period of 'periglacial fever', when there was unprecedented growth in laboratory experiment and quantitative process monitoring in the field. Research by Rapp (1960) in Kärkevagge, a valley in the alpine zone of of northern Sweden, was a milestone in this regard. For nine years, he monitored the frequency and magnitude of a wide spectrum of landscape processes using innovative field methods. Unexpectedly, his quantitative estimates showed generally low levels of activity and a minor role for frost weathering, solifluction and rapid mass movement, and the predominance of chemical weathering and fluvial transport as denudational processes. From the 1980s to the 1990s, field monitoring, combined with laboratory experiments on frost weathering, challenged what André (2009) termed the 'freeze-thaw dogma'—the traditional view that frost weathering is the dominant periglacial process—and raised awareness of the importance of azonal processes in periglacial landscapes.

Although monitoring and experiment continue to make an indispensable contribution to understanding periglacial landscapes, these approaches have weaknesses, two of which will be briefly mentioned here. First, the early laboratory studies, such as those at the Centre National de la Recherche Scientifique, Centre de Géomorphologie, Caen, France, reviewed by Lautridou and Ozouf (1982), which involved the disintegration of small rock particles under frequent freeze-thaw cycles, did not replicate field conditions well. The large-calibre debris accumulations that characterise many Scandinavian and other periglacial landscapes must be caused primarily by deep penetration of the annual freeze-thaw cycle into bedrock (cf. Matsuoka 2001). Later experiments, such as those of Murton et al. (2001, 2005), used sizable blocks of rock (450 $\times$ 300 $\times$ 300 mm) and were therefore closer simulations of conditions in the field. Linked to this was the lack of appreciation of the restricted areas of the landscape where frost shattering or frost wedging is important, namely areas of water availability. Thus, frost weathering can be slight on well-drained glacially-scoured rock outcrops, yet take place efficiently on adjacent cliffs subject to groundwater seepage. Second, field-monitoring studies in particular catchments over a small number of years are extremely problematic when attempting to scale-up in space and extrapolate in time. It is clear, therefore, that periglacial landscapes cannot be understood by reference to present processes alone.

Over time, Quaternary geology and other Quaternary sciences have provided the missing link. In Scandinavia, closer connections between periglacial geomorphology and the Quaternary sciences were being established in the closing decades of the twentieth century with a growing awareness of the effects and legacy of Pleistocene (Kleman 1992, 1994; Sollid and Sørbel 1994) and Holocene (Karlén 1988; Nesje and Kvamme 1991; Nesje et al. 1991; Matthews and Karlén 1992) environmental change. Although these insights originated from glacial geology and glacial geomorphology, they are equally applicable to the periglacial domain (as will be demonstrated later in this chapter).

2.3 Early Twenty-First Century Advances

Quaternary science diversified the techniques and approaches available for investigating periglacial landscapes. Foremost amongst these is a battery of numerical dating techniques. In combination with mapping and stratigraphic approaches, accurate and precise dating enables the reconstruction of landscapes of the past with high temporal resolution and also allows the separation of active from relict elements in the present landscape. Amongst the growing number of dating techniques available, Accelerator Mass Spectrometry radiocarbon dating, in situ cosmic-ray exposure-age dating, luminescence dating and Schmidt-hammer exposure-age dating have been found particularly useful in periglacial landscapes, where organic material is limited and bedrock outcrops and boulder deposits are abundant.

Other relatively new technical developments that are having a profound influence on research into periglacial landscapes in the twenty-first century include the use of geophysical survey, boreholes, satellite remote sensing such as light detection and ranging (LiDAR), airborne and terrestrial synthetic aperture radar interferometry (InSAR), computer algoritms for photogrammetry (structure from motion software), geographical information systems, and numerical and physical modelling. This is well illustrated in relation to the significant progress that has been made in understanding the nature, distribution and significance of permafrost in Scandinavia. Both French (2018) and Harris et al. (2018) define geocryology as the science of permafrost which, in respect of its core techniques, approaches and engineering aspects, may be considered as part of geophysics. Field studies using geophysical surveying of permafrost and ground temperature measurements began in both the northern and southern alpine areas in the 1980s (King 1984). Thirty boreholes were established in the International Polar Year, 2007–2009 (Christiansen et al. 2010). Data from boreholes were integrated with daily temperature and snow cover data in the CryoGRID1 model at 1 km^2 resolution, culminated in the first detailed and reliable permafrost map for Norway, Sweden and Finland (Gisnås et al. 2017).

Thus, today's studies of periglacial landscapes increasingly involve merging the research traditions of periglacial geomorphology, Quaternary science and geocryology (Harris and Murton 2005; Etzelmüller and Hagen 2005; French and Thorn 2006). Recent progress in dating periglacial features, obtaining chronological constraints, and positioning them in the palaeoclimatic context, have been particularly important. Like most fields of study focusing on the natural world, research programmes are being directed towards the climate change agenda in response to concerns over global warming (André 2009; Harris et al. 2009; Berthling et al. 2013; Etzelmüller et al. 2020). In Scandinavia where, due to polar amplification, atmospheric warming is likely to be above average, the importance of global climatic issues such as degrading permafrost, and its impacts on geohazards, carbon budgets, conservation and sustainability (e.g. Harris et al. 2009; Aalto et al. 2014; Karjalainen et al. 2019, 2020; Etzelmüller et al. 2020, 2021), are only likely to increase in the future.

3 Landforms, Processes and Age

Periglacial landscapes are commonly defined as the landforms and geomorphological processes characteristic of non-glacial cold climates (cf. Washburn 1979; Seppälä 2005a; Humlum 2008; Ballantyne 2018; French 2018; Murton 2021). The landforms bear an imprint of the processes of weathering, erosion and deposition associated with the freezing and thawing of ice in the ground (bedrock or regolith). However, landscapes in non-glacial cold-climates are also affected by river, lake and coastal ice, groundwater, snow and wind, all of which must be taken into accunt. Furthermore, periglacial and glacial landforms may be affected by transitional processes on different temporal scales, which leads to questioning the feasibility of strict differentiation.

Our aim is therefore to summarise and synthesise current knowledge of the periglacial landscapes of Scandinavia, pointing out their distinctive aspects in the context of Europe, and highlighting some unresolved research problems. Within this broad aim our approach is to focus on how and when the landforms evolved towards their present state. We examine plateau, steepland, low-gradient and glacier-foreland landscapes, the characteristic landforms of each having developed in response to periglacial processes under different topographic and other controls in the face of continuing environmental change. Owing to the scale of Scandinavia there is also the need to focus on exemplary and well-studied regions.

3.1 Plateau Landscapes

During Pleistocene interglacials, the high mountain and plateau landscapes of Scandinavia are likely to have experienced periglacial regimes similar to those of today. The dominant glaciation mode in the Scandes during glacials involved ice sheets and ice caps smaller than those of the Last Glacial Maximum with many plateau landscapes (along with the landscapes of the coasts and lowlands) subaerially exposed (not covered by LGM-like ice) and subjected to very cold periglacial climates (Porter 1989; Fredin 2002; Kleman et al. 2008). What are the implications of this history for the evolution of these periglacial landscapes? Recent debate has focused on the age and origin of blockfields and associated landforms on the plateaux, including whether they are wholly periglacial in origin, the role of frost weathering, whether they are in equilibrium with present environmental conditions, the extent of glacial erosion, and the possibility that these landforms could be pre-Pleistocene relicts.

3.1.1 Blockfields

Autochthonous (in situ) blockfields occur on low-angle plateau surfaces and mountain tops throughout the Scandes and are particularly extensive in present continuous and discontinuous permafrost zones (Rudberg 1977; Nesje et al. 1988; Juliussen and Humlum 2007; Goodfellow et al. 2014; Marr and Löffler 2018; Marr et al. 2018; Andersen et al. 2019). They seem typically to be composed of subangular to subrounded boulders at the surface (Fig. 3a), beneath which occur diamictons with more angular material, a sand or silt-sand matrix, and low clay content. The regolith seems normally to be up to several metres deep but excavations to bedrock have rarely been reported. A high proportion of the surface area of some blockfields is characterised by large sorted circles, transitioning to sorted stripes on sloping terrain (see Sect. 3.3.1).

Three main hypotheses for blockfield origin, development and survival have been proposed, suggesting they formed: (1) since deglaciation under periglacial climatic conditions similar to those existing today; (2) during Pleistocene periglacial climatic episodes and survived being overridden by one or more cold-based ice sheets; or (3) before the Pleistocene under a non-periglacial climatic regime and survived later episodes of glaciation (see, for example, Ballantyne 2010). The second hypothesis has been favoured by recent research and is exemplified by the results of 141 cosmic-ray exposure-age dates from regolith depth profiles, boulder erratics and bedrock outcrops combined with inverse modelling and sedimentological analysis of data from regolith profiles from the plateau landscape in Reinheimen National Park, central southern Norway (Andersen et al. 2019). Apparent ^{10}Be exposure ages for bedrock samples ranged from 78.0 ± 7.0 to 7.5 ± 0.7 ka with age clusters at ~11.0 and ~30.0 ka. The dates from the regolith profiles ranged between ~67.0 and 11.0 ka, and erratic boulders in the blockfield were dated to ~10.5 ka. The dates from erratics are fully consistent with deglaciation of the plateau in the early Holocene whereas the earlier dates from bedrock and regolith profiles demonstrate that parts of the blockfield fabric survived glaciation, including the Last Glacial Maximum (~22.0–21.0 ka). These ages demonstrate that blockfield formation in Reinheimen could not have begun post-Pleistocene, but appear not old enough to support a pre-Pleistocene origin.

Previous studies had suggested that the degree of chemical weathering indicated by the presence of secondary minerals, such as gibbsite and kaolinite, and high clay and fine silt contents in some blockfields might be the result of pre-Pleistocene weathering under a warm humid climate (e.g. Rea et al. 1996; André 2003; Paasche et al. 2006; Strømsøe and Paasche 2011; Olesen et al. 2012). However, Goodfellow (2012) and Goodfellow et al. (2014) have argued that low clay: silt ratios from blockfield matrix indicate the dominance of physical (frost) weathering, and that small amounts of secondary minerals result from chemical weathering in a cold climate under favourable hydrological conditions provided by a seasonally-wet active layer overlying permafrost. Furthermore, in situ cosmogenic nuclide concentrations measured in the regolith depth profiles by Andersen et al. (2019) indicate Reinheimen plateau summit erosion rates of ~6–8 m per Ma, increasing downslope. In contrast, the Last Glacial Maximum ice sheet was more erosive on the lower-lying plateaus towards its western margin (such as those surrounding the Sognefjord), where blockfields are

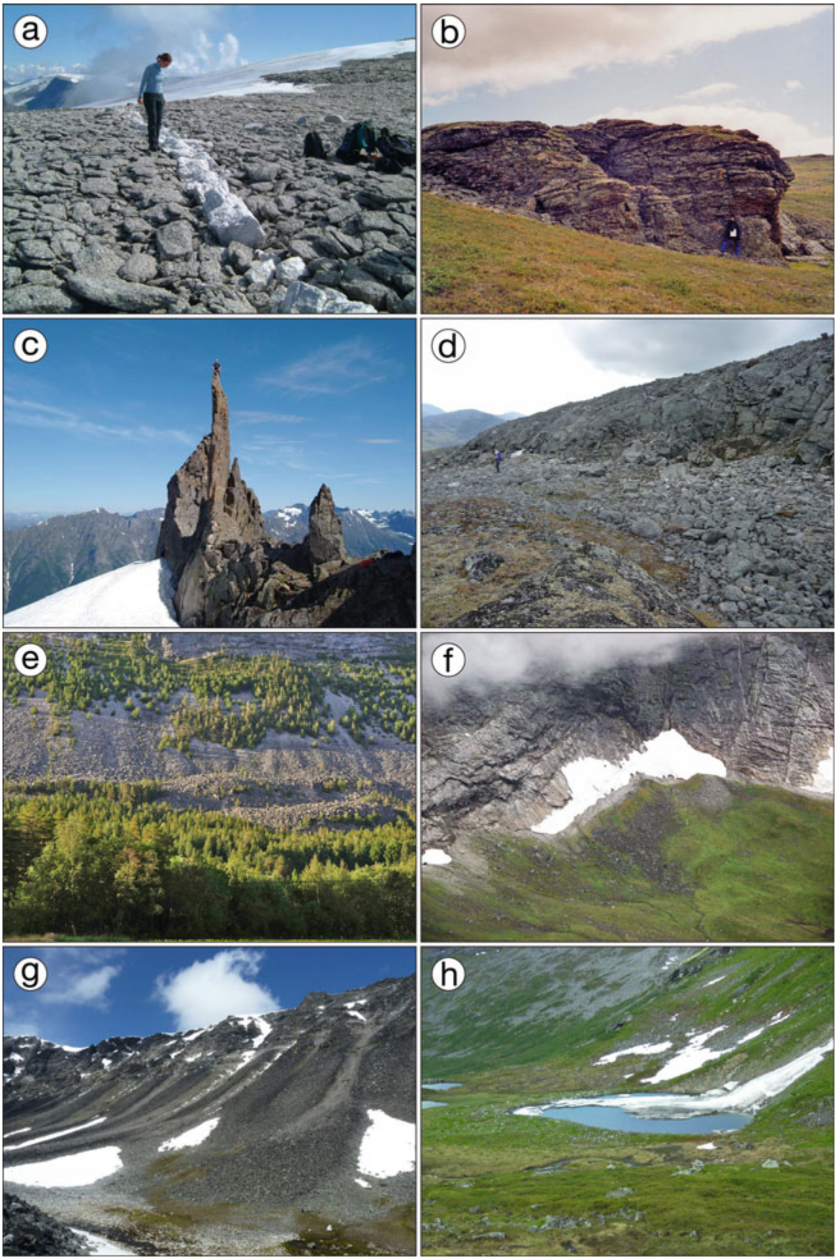
a
b
c
d
e
f
g
h

◀**Fig. 3** Selected periglacial landforms in Scandinavia. **a** Autochthonous blockfield with prominent quartzitic vein and scattered erratics, Melheimfjellet, Olden, western Norway (photo: Atle Nesje). **b** Highly weathered granulite tor, Paistunturi, northern Finland (photo: Jan Hjort). **c** Frost-shattered rock pinnacle ('The Blade'), Molladalen, Sunnmøre, western Norway (photo: Mons Rustøy). **d** Cryoplanation terrace, Svartkampan, Jotunheimen, southern Norway (photo: Richard Mourne). **e** Talus-derived rock glacier, Øyberget, Ottadalen, southern Norway (photo: Stefan Winkler). **f** Pronival rampart, Smørbotn, Romsdalsalpane, southern Norway (photo: Peter Wilson). **g** snow-avalanche boulder fan, Trollsteinkvelven, Jotunheimen, (photo: Jennifer Hill); **h** snow-avalanche impact crater, Meiadalen, Romsdalsalpane, western Norway (photo: John Matthews)

absent (Andersen et al. 2018). The evidence is therefore consistent with extremely slow lowering of the inland plateau surface by frost weathering where inefficient erosional processes dominated by frost creep, resulted in smooth, parabolic summits with occasional residual rock outcrops remaining as tors.

3.1.2 Tors and Rock Pinnacles

The widespread distribution of well-developed tors near the central area of glaciation in northern Sweden and northern Finland indicates that these areas have been protected from glacial erosion during all glacial cycles since ice-sheet inception in the late Cenozoic (Hättestrand and Stroeven (2002). Based on cosmic-ray exposure-age dating, these tors have yielded minimum ages which, when adjusted for $^{26}Al/^{10}Be$ ratios and the likely time shielded by ice sheets, suggests that this element of the landscape has survived as many as 14–16 episodes of glaciation (Fabel et al. 2002; Strøeven et al. 2002; Darmody et al. 2008). The highly weathered nature of the tors that rise above blockfields (Fig. 3b) can be attributed to relatively slow chemical weathering rates of resistant bedrock, the surface of which constitutes an exposed micro-environment with relatively low moisture availability (Darmody et al. 2008). The evidence seems to confirm the low weathering rates of exposed bedrock in a very old periglacial landscape. However, whereas resistant tors may survive multiple glaciations, the surrounding regolith of the blockfield elements of the landscape probably survived many fewer, perhaps only one or two. Sorted patterned ground that decorates the surface of many blockfields, and rare examples of blockstreams (Wilson et al. 2017), are the elements of these landscapes that are least likely to have survived glaciation, due to their greater sensitivity to warm-based glaciers during the transition from glacial to interglacial conditions.

At relatively low altitudes close to the west and north coasts of southern Norway, and in the Lofoten-Vesterålen archipelago of northern Norway, some tors and blockfields may not have been overridden by ice sheets during the Last Glacial Maximum and, by implication, earlier glaciations (Paasche et al. 2006; Nesje et al. 2007). Here, according to the 'Kleman model', warm-based ice streams descending steeply from the Scandes, eroded deep valleys and fjords, without overtopping the highest plateau surfaces and mountain summits (Nesje and Willans 1994; Kleman et al. 2008;

Strømsøe and Paasche 2011). This model is supported by an extensive, possibly ice-marginal trimline at ~250 m a.s.l. on the islands of Langøya and Hadseløya, which separates the 'glacial' landscapes from the 'periglacial' landscapes above (Paasche et al. 2006).

Perhaps the most distinctive landforms of periglacial landscapes throughout the coastal mountains of the Norwegian west coast are the jagged rock pinnacles that characterise the highest summits and ridges (Fig. 3c) and likely bear witness to uninterrupted frost weathering during glacial episodes (including the Last Glacial Maximum) when they appear to have been exposed as nunataks above the ice-sheet surface (Nesje et al. 1988). Such pinnacles are absent from inland mountains that were covered by the cold-based, central parts of ice sheets.

3.1.3 Cryoplanation and Nivation

Processes of cryoplanation have been proposed as a possible alternative to creep-dominated processes in the denudation of periglacial mountain and plateau landscapes (e.g. Demek 1969; Priesnitz 1988; Lauriol et al. 2006; Nyland et al. 2020). The most commonly cited evidence for the existence of cryoplanation is cryoplanation terraces, which are typically near-horizontal bedrock surfaces or benches backed by frost-weathered bedrock cliffs (Fig. 3d).

A recently proposed conceptual model of cryoplanation terrace formation in the alpine permafrost zone at Svartkampan, Jotunheimen, southern Norway (Matthews et al. 2019), develops the ideas of Boch and Krasnov (1943) on landscape evolution driven by frost weathering. Seasonal groundwater flow towards the freezing front in the cliff enhances frost weathering at the cliff-terrace junction, undermining and maintaining a near vertical cliff. Combined with the inefficient evacuation of regolith across the terrace tread by solifluction, this leads to parallel retreat of the cliff and terrace extension. Schmidt-hammer exposure-age dating of the bedrock cliffs and boulders embedded in the terrace surfaces at Svartkampen revealed Holocene ages ranging from modern to 8.9 ± 1.2 ka. Radiocarbon ages of up to ~5000 cal years BP were obtained from palaeosol material buried in the regolith at only 1.1–2.1 m from the cliff base, indicating *maximum* cliff recession rates of ~0.1 m per ka. Thus, cryoplanation at the site was shown to be a very slow process, incompatible with formation of the terraces entirely since deglaciation but compatible with their possible survival beneath cold-based ice sheets. It should be pointed out, however, that cryoplanation terraces do not appear to be common enough for cryoplanation to have had more than a minor influence on late-Pleistocene landscape evolution in the Scandinavian context.

Perhaps more common and often confused with cryoplanation is nivation, which comprises processes enhanced by the presence of late-lying snowbeds (Thorn 1988; Nyberg 1991; Hall 1998; Thorn and Hall 2002; Margold et al. 2011). It includes the enhancement of chemical weathering in water-saturated sediment and the transport of sediment by solifluction and meltwater flow from beneath a snowbed, but does not include frost weathering of bedrock. This is the main process involved in the formation of cryoplanation terraces but does not appear to be enhanced beneath snowbeds (see discussion in Matthews et al. 2019). Nivation can, however, produce nivation benches (or nivation hollows) in hillslopes covered in regolith (Christiansen 1998). Such benches may be fronted by solifluction lobes (see below) and/or stone pavements (surficial lag deposits resulting from the removal of the fine matrix sediment by slope wash). Little recent research has been carried out on nivation or nivation benches in Scandinavia (but see Rapp 1984; Rapp and Nyberg 1988). The only dated example from Scandinavia known to the authors is from Söderåsen, southern Sweden, where luminescence dates on aeolian sand on the surface of a nivation bench yielded Younger Dryas ages (Jonasson et al. 1997), which indicate a relict feature.

3.2 Steepland Landscapes

The term 'steepland' was introduced by Slaymaker (1995) to denote landscapes characterised by steep gradients, which profoundly influence mass movement processes. In this section, we focus on periglacial steeplands, the evolution of which in Scandinavia includes distinctive paraglacial and paraperiglacial aspects. Paraglacial processes are non-glacial processes directly conditioned by glaciation (Church and Ryder 1972; Ballantyne 2002; Slaymaker 2009) and include, for example, rock-slope failure in response to glacio-isostatic uplift or glacial de-buttressing. Paraperiglacial processes, which have been defined as non-permafrost processes directly conditioned by permafrost (Mercier 2008; Scarpozza 2016), include slope failures in both bedrock and regolith triggered by thawing permafrost. The concepts of periglaciation, glaciation, paraglaciation and paraperiglaciation are linked by the concept of cryoconditioning (Berthling and Etzelmüller 2011), important aspects of which include the thawing of ice associated with bedrock and sediments beneath cold-based glaciers, as well as the changing availability of meltwater to both groundwater and surface-water flows during and following deglaciation.

3.2.1 Rock-Slope Failures

Retreat of the Scandinavian Ice Sheet from its limits at the Last Glacial Maximum and in the Younger Dryas (Fig. 1) led to a large number of rock-slope failures in the steeplands of southern and northern Scandinavia, many of which have been dated using cosmic-ray exposure-age dating (e.g. Blikra and Christiansen 2014; Böhme et al. 2015; Hermanns et al. 2017; Oppikofer et al. 2017; Schleier et al. 2017; Hilger et al. 2018, 2021; Wilson et al. 2019; Curry 2021).

Several data sets have been compiled to examine the spatial distribution and/or temporal frequency of rock-slope failures in relation to the time elapsed since deglaciation in southern Norway. Hermanns et al. (2017) found nearly half of 22 accurately dated large rock avalanches occurred within 1.0 ka of deglaciation. The

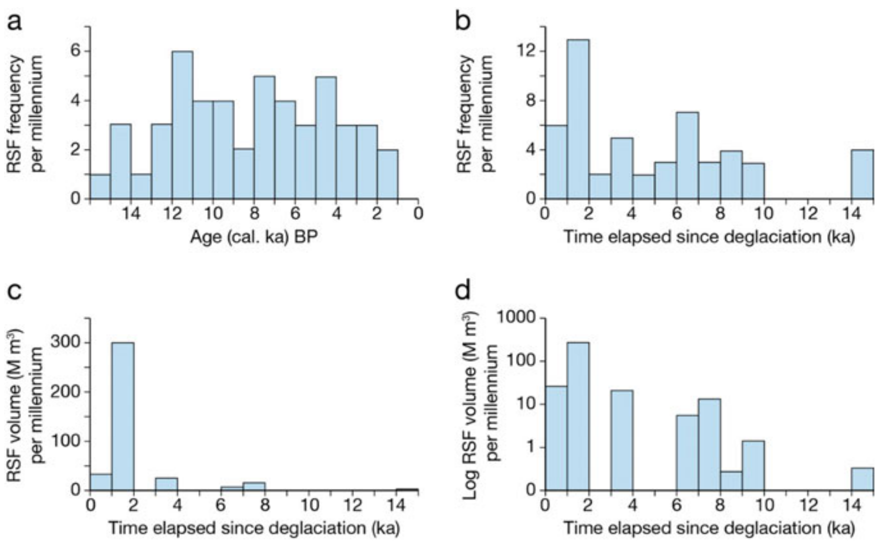

Fig. 4 Frequency and magnitude of moderate to large rock-slope failures (RSFs) in western Norway per millennium 16–0 ka: **a** age-frequency of RSFs; **b** frequency of RSFs related to time elapsed since local deglaciation; **c** volume of RSFs related to time elapsed since local glaciation; **d** volume of RSFs related to time elapsed since local deglaciation with volume on a logarithmic scale (based on Curry 2021)

larger data set of 49 moderate to large rock-slope failures compiled by Curry (2021) shows almost 40% of events occurred within 2.0 ka of deglaciation (Fig. 4). A similar, dominant activity peak is clear in even larger data sets of >100 events compiled by Longva et al. (2009), Böhme et al. (2015; Fig. 5a) and Bellwald et al. (2019), which include data derived from seismic stratigraphy of fjord sediments.

All these records give some indication of one or more secondary peaks or clusters in the frequency of events in the mid- to late Holocene, which may relate to century- to millennial-scale climatic variations. This is suggested in Fig. 5a by the small increase in the frequency of events from ~5.0–1.0 ka, which correlates with the fall in temperature and rise in precipitation during neoglaciation after the Holocene Thermal Maximum (Figs. 5j, k). Other temporal clusters of rock-slope failures have been tentatively identified, such as at ~5.0 ka (Hilger et al. 2018), and ~5.0–4.0 ka and ~8.0–7.0 ka (Curry 2021; Fig. 4), but the significance of such clusters is uncertain.

The concentration of rock-slope failures close in time to deglaciation points to several potential paraglacial trigger factors, including ice-sheet thinning, debuttressing of oversteepened glaciated valley slopes, and glacio-isostatic seismic shock. Those that occurred later in the Holocene may have involved progressive failure and/or transient triggering mechanisms. Historical rock-slope failures in Møre og Romsdal exhibit evidence of spatial clustering in the area of greatest current land-uplift rates, with the highest number of occurrences at a distance of 60–80 km from the Norwegian west coast (Henderson and Saintot 2011; Curry 2021), which suggests

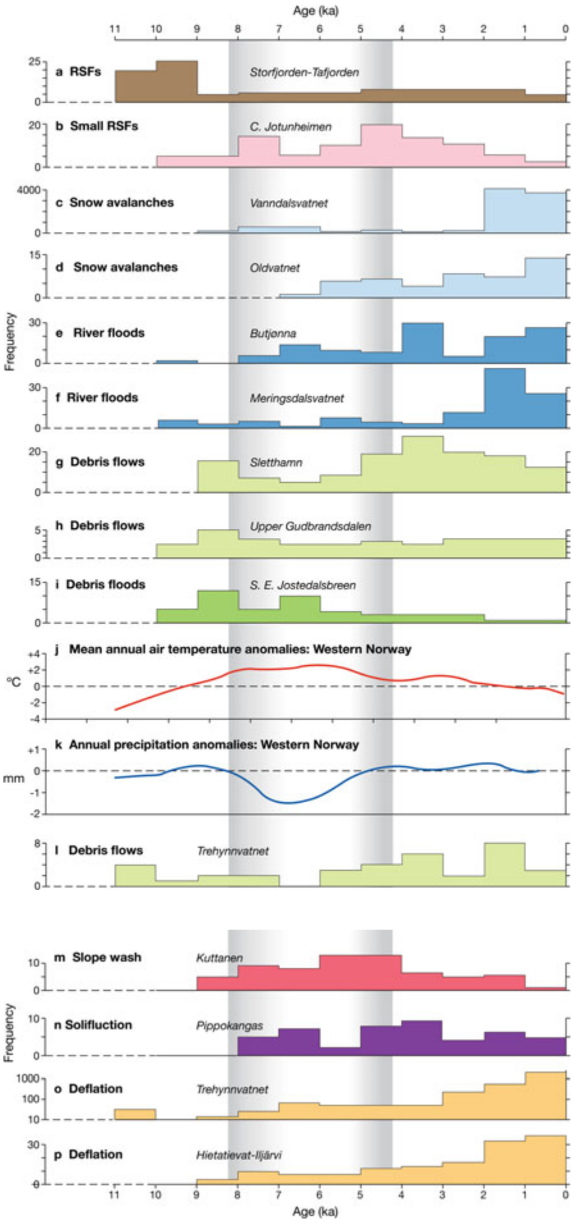
Age (ka)
a RSFs
Storfjorden-Tafjorden
b Small RSFs
C. Jotunheimen
c Snow avalanches
Vanndalsvatnet
d Snow avalanches
Oldvatnet
e River floods
Butjønna
f River floods
Meringsdalsvatnet
g Debris flows
Sletthamn
h Debris flows
Upper Gudbrandsdalen
i Debris floods
S. E. Jostedalsbreen
j Mean annual air temperature anomalies: Western Norway
k Annual precipitation anomalies: Western Norway
l Debris flows
Trehynnvatnet
m Slope wash
Kuttanen
n Solifluction
Pippokangas
o Deflation
Trehynnvatnet
p Deflation
Hietatievat-Iljärvi
Frequency
°C
mm

◀**Fig. 5** Holocene chronologies of the activity of landforms and geomorphic processes in the landscapes of southern (**a**–**i**) and northern (**l**–**p**) Scandinavia, in relation to climatic variations (**j**–**k**). All records except (**c**) and (**n**) depict frequency of events per millennium. Early-, mid- and late-Holocene subdivisions of the Holocene are shown according to Walker et al. (2018). **a** Rock-slope failures in the Storfjorden/Tafjorden region, based on cosmogenic exposure-age dating and fjord sediment stratigraphy (Böhme et al. 2015, n = 105). **b** Small rock-slope failures in central Jotunheimen, based on Schmidt-hammer exposure-age dating (Matthews et al. 2018, n = 92). **c**–**d** Snow avalanches from radiocarbon-dated lacustrine sediment stratigraphy: (**c**) Vanndalsvatnet, E Jostedalsbreen region, showing the number of particles > 1 mm (Nesje et al. 2007); (**d**) Oldvatnet, N Jostedalsbreen region (Vasskog et al. 2011, n = 49). **e**–**f** River floods from radiocarbon-dated lacustrine sediment stratigraphy: **e** Butjønna, upper Glomma catchment, Rondane region (Bøe et al. 2006; Nesje et al. 2007, n = 115); **f** Meringsdalsvatnet, E Jotunheimen (Støren et al. 2010, n = 108). **g**–**h** Debris flows from radiocarbon-dated colluvial stratigraphy: (**g**) Sletthamn, central Jotunheimen (Matthews et al. 2009, n = 123); (**h**) upper Gudbrandsdalen (Sletten and Blikra 2007, n = 64). **i** Debris floods from Schmidt-hammer exposure-age dating of surface boulder deposits on alluvial fans, SE Jostedalsbreen region (Matthews et al. 2020b, n = 47). **j**–**k** Climatic anomalies (smoothed) for the normal period AD 1961–91, western Norway (Mauri et al. 2015; Hilger et al. 2021): (**j**) mean annual air temperature (MAAT); (**k**) annual precipitation (AP). **l** Debris flows from radiocarbon-dated lacustrine stratigraphy at Trehynnvatnet, Vesterålen, northern Norway (Nielsen et al. 2016a, n = 35). **m** Slope wash from radiocarbon-dated colluvial stratigraphy at Kuttanen, Finnish Lapland (Matthews and Seppälä 2015, n = 131). **n** Solifluction from radiocarbon-dated lobe stratigraphy at Pippokangas, Finnish Lapland (Matthews et al. 2005, n = 46). **o** Deflation from radiocarbon-dated sand-dune stratigraphy in Finnish Lapland (Kotilainen 2004; Matthews and Seppälä 2014, n = 137). **p** Deflation as indicated by the number of sand grains >250 µm from radiocarbon-dated lacustrine stratigraphy at Trehynnvatnet, Vesterålen, northern Norway (Nielsen et al. 2016a, n = 35; note the logarithmic scale)

that long-lasting glacial-isostatic driven seismic paraglacial effects have remained important throughout the Holocene.

Many modern, historical and older large rock-slope failure events are associated with steep rock walls that contain permafrost today and/or are likely to have contained permafrost in the past (Magnin et al. 2019). Based on cosmic-ray exposure-age dating and permafrost modelling, the timing of deformation initiation and late-Pleistocene and Holocene sliding rates along slip surfaces were analysed for several actively deforming examples in northern and southern Norway (Hilger et al. 2021). At two sites (Oppstadhornet and Skjeringahaugane) without permafrost in the Holocene, deformation started shortly after local deglaciation at 16.0–14.0 and 11.0–10.0 ka, respectively. At three sites (Mannen, Revdalsfjellet and Gámanjunni), deformation started between 8.0 and 4.5 ka, during or at the end of the Holocene Thermal Maximum, when permafrost was most degraded. The evidence indicates that the presence of permafrost had a stabilising effect for several millennia after deglaciation and that sliding rates tended to decrease during the Holocene. In addition, modern measured sliding rates suggest recent acceleration at the three sites with permafrost, attributed to further permafrost degradation in response to recent climate warming. Hilger et al. (2021) concluded that permafrost degradation should be regarded as a first-order control on the stability and activity of steep rock slopes.

The importance of permafrost degradation has been further highlighted in an analysis of 92 small rock-slope failures in Jotunheimen ranging in volume from 12 to 2520 m^3, which have been dated by Schmidt-hammer exposure age dating (Matthews et al. 2018). These landforms comprise compact depositional fans of predominantly angular boulders beneath distinct erosional scars in bedrock cliffs. They were located at or close to the aspect-dependent lower limit of discontinuous permafrost in alpine rock faces as defined by Hipp et al. (2014). Age-frequency and probability-density analyses revealed low early-Holocene activity increasing to a dominant mode at 4.5 ± 1.4 ka (Fig. 5b). The increase in activity during and especially towards the end of the Holocene Thermal Maximum differs markedly from the paraglacial pattern exhibited by larger rock-slope failures. By combining this chronology with permafrost depth modelling, Matthews et al. (2018) revealed that peak activity was associated with minimum permafrost depth (maximum active-layer thickness) close to the end of the Holocene Thermal Maximum. This is essentially a paraperiglacial response. Earlier secondary activity phases seem to have represented earlier pulses of permafrost degradation. The continuous decline in activity after ~4.5 ka may signify the exhaustion of permafrost at depths shallow enough to host small rock-slope failures. A further reduction in activity would be expected in response to permafrost aggradation in the Little Ice Age (cf. Lilleøren et al. 2012).

3.2.2 Talus Slopes and Rockfalls

Several colluvial landforms develop at the foot of steep rock slopes due largely to the accumulation of rockfall debris. The most common of these landforms are talus slopes, which typically consist of sheets or cones of coarse, angular rock debris, the steep surface gradient of which (~33–39°) lies close to the angle of repose of the debris, at least in the straight upper parts of the slope. However, debris-mantled slopes, characterised by a thinner mantle of debris with a lower surface gradient reflecting that of the underlying terrain, are far more common than mature talus slopes in Scandinavia.

There are several reasons for the contrast with many other European steepland landscapes, where talus slopes are more abundant. First, many areas of the Scandes with permafrost or seasonal frost, where enhanced sediment supply from frost weathering would be expected, are characterised by plateau topography, which lacks the necessary steep bedrock slopes and is largely seismologically inactive. Second, much of the largely metamorphic bedrock in Scandinavia is resistant to weathering in general and to frost weathering in particular. The best developed talus slopes are associated with frost-susceptible, well-jointed rocks such as the quartzitic sparagmites of the Rondane massif, southern Norway (Sellier and Kerguillec 2021). Third, in most of the Scandinavian steeplands, insufficient time has been available for the development of mature talus slopes under the climatic regime of the Holocene; and only a few thousand years longer has been available in the peripheral areas deglaciated before the Younger Dryas. Fourth, although there is the possibility that inland talus slopes could have survived glaciation beneath cold-based ice sheets, the steepland areas towards the coast tend to have been scoured by ice streams during successive glaciations.

Rapp (1957, 1960) suggested, on the basis of his classic process-monitoring studies, that modern rockfall activity in the alpine valley of Kärkevagge, northern Sweden, is very limited, the talus slopes largely relict, and talus accumulation probably greatest shortly after deglaciation. This view of the evolution of talus slopes seems to be generally applicable in Scandinavia, even in areas most conducive to frost weathering, such as Rondane.

This paraglacial hypothesis for talus slope development in Scandinavia has been substantiated and the timing of talus accumulation clarified by stratigraphical studies. Blikra and Nemec (1998) dated colluvial sequences beneath coastal cliffs over a wide area of the outer coastal zone of Møre og Romsdal in southern Norway. They identified main stratigraphic units (A–C) separated by hiatuses, which represent a five-stage (1–5) evolution of what they termed 'rockfall-dominated colluvial-fan deltas' (Fig. 6). Unit B, consists of openwork rockfall boulders and cobbles (talus) alternating with low-viscosity debris-flow cobbles and pebbles (reworked talus). Within this talus unit, a frost-shattered palaeobeach facies lies at the height of a Younger Dryas shoreline, which effectively dates the main phase of talus accumulation and confirms a periglacial climate at sea level. Unit A (stage 1) consists of matrix-rich gravels, interpreted as high-viscosity debris flows (resedimented till), almost concurrent with local deglaciation, at a time of higher relative sea level and in a climate less conducive to frost weathering than unit B. Unit C represents renewed talus deposition, similar to unit B apart from interbedded humic palaeosol material, which was radiocarbon dated, and suggests variations in the rate of rockfall activity during the second half of the Holocene (see also Blikra and Nesje 1997). The hiatuses indicate stages without rockfall activity both before the Younger Dryas (during the Allerød interstadial) and during the early Holocene.

Unit B (Younger Dryas) dominates the stratigraphy and is significantly younger than unit A, which is a paraglacial feature. This suggests that rockfall-talus accumulation at this sea-level location was related to the climate of the Younger Dryas, rather than simply to paraglacial instability. Further support for climatic control of talus-slope development comes from late-Holocene variations in rockfall activity on talus slopes dated by lichenometry and further analysed by simulation modelling in Jotunheimen (McCarroll et al. 1998, 2001). These authors demonstrated that the rate of rockfall-talus accumulation in the eighteenth century, the coldest phase of the Little Ice Age, may have been at least five times the background late-Holocene rate.

3.2.3 Rock Glaciers

In their inventory based largely on aerial photographic interpretation, Lilleøren and Etzelmüller (2011) recognized 241 rock glaciers in Norway, 85% of which are in the north of the country. Barsch and Treter (1976) had previously identified a small number of rock glaciers at the foot of prominent talus slopes in Rondane, southern Norway, while Sollid and Sørbel (1992) recognised the relatively large number of

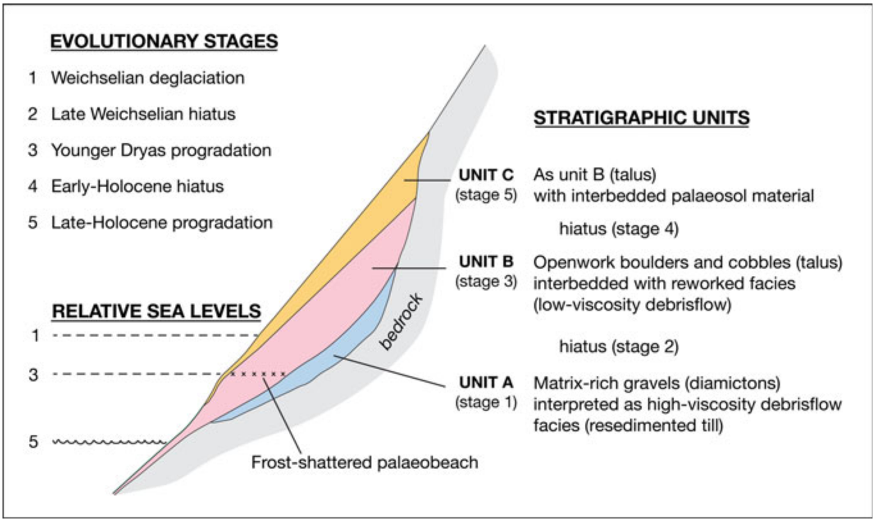

Fig. 6 Stratigraphic model of a 'rockfall-dominated colluvial-fan delta' in coastal Møre og Romsdal, southern Norway. Three stratigraphic units separated by hiatuses are assigned to five evolutionary stages and associated with three different relative sea levels. Note also the frost shattered palaeobeach in unit 2 at the Younger Dryas sea-level stand (based on Blikra and Nemec 1998)

rock glaciers in northern Norway outside Younger Dryas glacier limits, some of which occur close to sea level.

Lilleøren and Etzelmüller (2011) distinguished between talus- and moraine-derived rock glaciers, the former exhibiting evidence of permafrost creep at the foot of talus slopes (Fig. 3e), the latter derived from glacigenic sediments at locations below cirque glaciers. In northern Norway, their data included 188 talus-derived and 18 moraine-derived rock glaciers; in southern Norway, only 23 talus-derived and 12 moraine-derived rock glaciers were identified. The limited number of rock glaciers in southern Norway can be explained by similar reasoning to that proposed above for the sparsity of mature talus slopes—namely, insufficient sediment supply under a permafrost regime for development of such features beneath steep rock walls in a plateau landscapes. Lilleøren and Etzelmüller (2011) also attempted to distinguish between active and relict features but their 'intact' rock glaciers cannot be regarded as equivalent to 'active' ones. Morphological criteria such as steep frontal slopes, and deep ridges and furrows, are not reliable indicators of activity because of the potential for the persistence of such attributes in the landscape long after activity ceases. Active rock glaciers have been recently proven at Ádjet, Troms County, northern Norway by application of satellite InSAR measurements (Eriksen et al. 2018). Nevertheless, there can be little doubt, on the basis of the distribution and altitude of these landforms in non-permafrost zones, that most of the identified rock glaciers in both northern and southern Norway are relict.

There have been very few attempts to date rock glaciers in Scandinavia. Based on lacustrine sedimentary signals in Trollvatnet (Lyngen, northern Norway) a talus-derived rock glacier located at ~100 m a.s.l. formed following local deglaciation at >14.8 ka (Paasche et al. 2007). A steady sediment supply to the lake indicated that this rock glacier remained active until ~11.1 ka, becoming relict shortly after the end of the Younger Dryas, which coincided with the cessation of permafrost conditions. In southern Norway, both Schmidt-hammer and cosmic-ray exposure-age dating led to similar conclusions in relation to lobate, talus-derived rock glaciers at Øyberget, Ottadalen (Matthews et al. 2013; Linge et al. 2020). However, InSAR measurements have demonstrated that the Øyberget rock glaciers are active (Nesje et al. 2021) despite their location at ~530 m a.s.l. beneath south-facing rock walls and >1000 m below the lower limit of discontinuous permafrost, and having yielded dates up to 10.3 ± 1.3 and 11.2 ± 1.4 ka according to the two dating techniques, respectively. At this site, permafrost creep seems to have been initiated in the early Holocene as large quantities of paraglacial debris were released from the Øyberget rock wall. Sporadic permafrost developed and persisted in the blocky openwork sediments as a result of microclimatic undercooling mechanisms such as Balch ventilation and the chimney effect.

3.2.4 Ice-Cored Moraines

Another controversial issue related to rock glaciers in Scandinavia is their relationship to ice-cored moraines, which were investigated in detail for the first time in the 1950s (Østrem 1959, 1964, 1965). Ice-cored moraines are multiple-ridged, ramp-like structures that rise up to ~50 m above the surrounding terrain. They are most commonly located in the continuous or discontinuous permafrost zones of southern Norway where they are associated with small polythermal glaciers in relatively continental climatic regimes. Lilleøren and Etzelmüller (2011) recognised 26 ice-cored moraines in northern Norway and 40 in southern Norway, all of which were classified as intact/active permafrost indicators.

Barsch (1971, 1977) considered that ice-cored moraines *are* rock glaciers and interpreted the individual ridges as rock-glacier flow structures. Østrem (1971) argued that their position close to glacier fronts, their lack of movement, and their existence on level or near-level plateaux indicate glacial rather than mass-movement (permafrost creep) origins. Shakesby et al. (1987) and Matthews et al. (2014) supported Østrem's interpretation citing especially the lack of deformation induced by gravity. They considered that ice-cored moraine ridges are deposited and deform as a result of glacier-push processes during glacier advances. Hence, they used the term 'push-deformation moraine', which emphasises glacier push as the primary morphogenetic mechanism. However, the type of deformation exhibited by Scandinavian ice-cored moraines seems similar to rock-glacier creep and to be dependent on a permafrost environment (cf. Etzelmüller and Hagen 2005).

Matthews et al. (2014) applied Schmidt-hammer exposure-age dating to individual ridges within three ice-cored moraine complexes in Jotunheimen and Breheimen, southern Norway. At Gråsubreen, the ages of six ridges ranged from 3.9 ± 0.8 ka to modern and the outer ridges tended to be oldest; at Vesle Juvbreen both ridges yielded modern ages; and at Østre Tundradalskyrkjabreen, Breheimen, all four ridges dated to ~2 ka. These ages indicate significant activity during the late Holocene, which contrasts with the relict status of most rock glaciers in Scandinavia. The absence of older dates is explained by late-Holocene (including Little Ice Age) glacier advances, which reworked the moraine ridges, incorporating previously weathered boulders.

3.2.5 Pronival Ramparts

The defining characteristic of a pronival rampart is that it is formed at the distal margin of a snowbed. Some pronival ramparts occur at the foot of talus slopes but, as others abut directly against rock walls (Fig. 3f), the older term ‘protalus rampart’ is not appropriate (Shakesby 1997). Similarly, lack of generality leads to rejection of the idea that pronival ramparts are embryonic rock glaciers (cf. Haeberli 1985; Scapozza et al. 2011; Kääb 2013). Many active pronival ramparts investigated in northern and southern Scandinavia cannot be embryonic rock glaciers because they are developing in seasonal frost environments, not permafrost zones (e.g. Harris 1986; Ballantyne 1987; Shakesby et al. 1987, 1995, 1999; Matthews et al. 2017a).

Where sufficient boulders have enabled Schmidt-hammer exposure-age dating of pronival ramparts in southern Norway, both active and relict examples have been identified (Matthews et al. 2011, 2017a; Matthews and Wilson 2015; Marr et al. 2019; Wilson et al. 2020). Ages of 14.6 ± 1.1 to 8.7 ± 1.1 ka were obtained from relict examples located beyond ice-sheet and local-glacier limits during the Younger Dryas, while active ramparts (mostly inside the limits) yielded ages of 7.7 ± 1.1 ka to modern. The largest of these pronival ramparts seem to have developed under a permafrost regime during the Younger Dryas, or earlier when rockfall supply was enhanced by paraglacial slope instabilities. The ramparts that remained active after the Younger Dryas did so under the seasonal-frost regime of the Holocene with likely reduced sediment supply. These conclusions are consistent with four luminescence dates of 10.8 ± 1.0 to 10.4 ± 1.0 ka obtained by Jonasson et al. (1997) on aeolian sand in two possible pronival ramparts from southern Sweden. All the dating results are consistent with the supposed main process of pronival rampart formation, which involves the supranival transport of frost-weathered rockfall debris across steeply-sloping snowbed surfaces.

3.2.6 Snow-Avalanche Landforms

Snow avalanches undoubtedly contribute debris and snow to the development of some talus slopes, rock glaciers and pronival ramparts. Several small-scale landforms provide evidence of snow-avalanche activity on avalanche-affected slopes, including scattered perched angular boulders, boulder lines, gravel clumps, beaded gravel ridges, debris horns and debris shadows (Blikra and Nemec 1998; Owen et al.

2006a). Snow avalanches have also produced larger-scale landforms that are uniquely attributable to snow-avalanche processes, including snow-avalanche boulder fans (Fig. 3g) and snow-avalanche impact landforms (Fig. 3h), both of which are well represented in Scandinavia.

Snow-avalanche boulder fans were first recognised by Rapp (1959) who described distinctive avalanche ‘roadbank tongues’ in northern Sweden, which differ appreciably from talus slopes and other colluvial accumulations beneath steep bedrock slopes. Well-developed snow-avalanche boulder fans tend to be flat-topped, elongated, steep-sided, coarse-debris accumulations that extend at a low angle towards valley floors. The momentum of snow avalanches carries debris farther from the foot of the slope than is the case with talus slopes, producing strong concave-upwards curvature to the fan surface. Debris is transported from snow-avalanche headwall source areas by chutes or gullies eroded in bedrock.

In the Scandinavian examples investigated in detail by Matthews et al. (2020a) from two areas of Jotunheimen, southern Norway, the source areas lie in the high-alpine zone affected by permafrost, whereas the depositional fans are in the mid-alpine zone of seasonal frost. Schmidt-hammer exposure-age dating of boulders from the distal fringe of 11 fans yielded ages ranging from 7.4 ± 1.0 to 2.3 ± 0.7 ka. Geographical information systems-based morphometric analysis showed that the volume of rock material was generally less than the volume of the chutes. Although some unweathered boulders on the fan surface indicated continuing low-level activity by non-erosive, largely dry-snow avalanches, it was inferred that the fans were deposited entirely within the Holocene, and mainly within the early- to mid Holocene. The excess volume of the chutes was accounted for by enhanced subaerial erosion in the Younger Dryas (and possibly earlier) when they appear to have been located on frost-weathered nunataks protruding above the ice-sheet surface. The majority of the debris within the fans is therefore of paraglacial origin, probably supplemented by later additions from permafrost degradation associated with the Holocene Thermal Maximum.

Snow-avalanche impact landforms have been described from both northern (Corner 1980) and southern Scandinavia (Liestøl 1974; Hole 1981; Blikra et al. 1994; Matthews and McCarroll 1994; Owen et al. 2006a; Matthews et al. 2017b). In the steeplands of western Norway, erosional and depositional landforms of this type include valley-floor craters (Fig. 3h), lacustrine craters (subaquatic craters eroded in lake-floor sediments close to lake shores), river-bank ramparts (mounds and ridges of sedimentary material excavated from the channel bed and deposited on distal river banks). They occur in greater numbers in Vestlandet (western Norway) than anywhere else on Earth (Matthews and Owen 2021). Fifty-two valley-floor and lacustrine craters described by Matthews et al. (2017b) had an average diameter of 85 m (range 10–185 m) and were located at the bases of steep valley-sides with gradients of 28°–59°. It seems that the combination of exceptionally high snow volumes (reflected in mean annual snowfall amounts of > 4 m in the avalanche source areas), a gradient of at least ~15° for the lowest 200 m of the avalanche track, and a flat valley or lake floor, are all necessary for the development of such well-developed craters.

The composition of the depositional landforms associated with snow-avalanche impact reflects the composition of the sedimentary material excavated and ejected from the craters. Sufficient boulders were available on five snow-avalanche impact ramparts in Sprongdalen and Jostedalen to enable Schmidt-hammer exposure-age dating (Matthews et al. 2015). These yielded ages of 3.6 $\pm$ 0.5 to 0.6 $\pm$ 0.3 ka for the ramparts as a whole, whereas the distal fringes yielded ages up to 5.4 $\pm$ 1.0 ka, indicating that parts of the distal fringes survived burial by later impact events. The estimated maximum age of the surface boulders (defined as the age exceeded by the oldest 5%) was determined as up to ~9.0 ka. On the basis of this evidence alone, the evolution of the ramparts must have occurred throughout the Holocene as a result of frequent snow-avalanche events.

Comparative modelling by Matthews et al. (2017b) of the kinetic energy required to form meteorite and snow-avalanche impact craters with a diameter of 85 m indicates that the kinetic energy at impact of a single snow avalanche (~3.1×10^9 J) is two orders of magnitude less than that involved in excavating an 85-m diameter meterorite crater (~1.3×10^{11} J). This result is consistent with the number of snow-avalanche events that excavated the Vestlandet craters, estimated from meteorological data and dendrochronological and lacustrine proxy records in neighbouring valleys. These records suggest recurrence intervals for large snow-avalanche events of between 15 and 155 years (Vasskog et al. 2011; Decaulne et al. 2014).

However, such calculations take no account of variations in the frequency of snow-avalanche activity through time, for which there is evidence from stratigraphic studies. Based on terrestrial colluvial stratigraphy, Blikra and Nemec (1993, 1998), Blikra and Selvik (1998) reported relatively high frequency of snow-avalanche events during the Younger Dryas, contrasting with low activity levels in the early Holocene. A very late peak in activity (within the last two millennia) is clear in the lacustrine records of Nesje et al. (2007; Fig. 5c) and Vasskog et al. (2011; Fig. 5d). A similar pattern, with a dominant late-Holocene peak, seems also to characterise records of river floods (Bøe et al. 2006; Nesje et al. 2007; Støren et al. 2010, 2014; Engeland et al. 2020; Figs. 5e, f), which suggests possible links to winter snowfall, storminess and spring snowmelt. In addition, lichenometric dating and simulation modelling of lichen-size frequency distributions from 12 snow-avalanche ramparts (Matthews and McCarroll 1994) indicated variations in avalanche frequency over recent centuries, related to variations in snow climate.

3.2.7 Debris Flows and Debris Slides

Debris flows—a type of rapid mass movement of water-saturated unconsodidated sediment—are common in steeplands throughout Scandinavia today. Rubensdotter et al. (2021) recognise two major morphological types—open-slope debris flows and channel-dependent debris flows—together with sub-types of the latter. Several palaeoenvironmental reconstructions provide evidence of variations in the frequency of debris flows through time (Jonasson 1991; Blikra and Nemec 1993, 1998; Blikra and Nesje 1997; Matthews et al. 1997a, 2009; Sandvold et al. 2001; Sletten et al. 2003;

Sletten and Blikra 2007; Støren et al. 2008; Nielsen et al. 2016a). Larger-scale slope failures in unconsolidated material, such as debris slides (Sutinen et al. 2014; Ojala et al. 2019), have also been recognised in Scandinavia but dating is often difficult and trigger factors are likely to be different and more akin to those of rock-slope failures. Ojala et al. (2019) show that debris slides in northern Finland are located within 35 km of known postglacial faults and that the size of the slides decrease with distance from the faults, providing evidence of seismic triggering (see also Sutinen et al. 2014). Debris slides, like debris flows, are not exclusively periglacial landforms, although seasonal thawing or permafrost degradation may be involved as trigger factors. Here we focus on debris flows.

In southern Norway, detailed Holocene radiocarbon-dated terrestrial stratigraphic records are available from Sletthamn, Leirdalen, Jotunheimen (Matthews et al. 2009; Fig. 5g), and the upper Gudbransdalen region, farther east in southern Norway (Sletten and Blikra 2007; Fig. 5h). The sediments at Sletthamn represent distal debris-flow facies (cf. Matthews et al. 1999), and are illustrated in Fig. 7. The longer record, from Trehynnvatnet on Langøya in Vesterålen, northern Norway (Nielsen et al. 2016a; Fig. 5l), is based on turbulent subaqueous density currents triggered by debris flows. All three records show significant levels of debris-flow activity throughout the Holocene, with evidence of reduced activity in the mid-Holocene at ~7.0–6.0 ka, at the end of the Holocene Thermal Maximum (although millennial-scale variations are less clear in the Gudbrandsdalen record).

Debris flows are initiated by the failure of water-saturated sediments, which Matthews et al. (1999, 2009) attributed at Sletthamn primarily to the failure of till-mantled slopes following intense summer and autumn rainfall events. Till-mantled slopes are also involved at the Gudbrandsdalen sites whereas slopes around Trehynnvatnet involve both till-mantled and reworked-colluvial slopes. Rainfall events seem to be the main climatic trigger factor for modern debris flows in western Norway, rather than spring snowmelt, which is more important in eastern Norway (Sandersen 1997). However, all three records of debris-flow activity were probably affected by both summer rainstorms and environmental conditions in the spring, when both snowmelt and active-layer thaw are potential trigger factors. It can be speculated that such conditions were less likely during the Holocene Thermal Maximum (when debris-flow activity was at a minimum) than before or after.

3.2.8 Alluvial Fans and Debris Floods

Water flows, debris floods, debris flows and slush flows commonly produce fans or fan-like landforms on the lower valley-side slopes and valley floors of periglacial steeplands. The special environmental conditions affecting these landforms in periglacial landscapes today include the seasonal availability of meltwater from snow, ice and frozen ground. Differentiation of such fans is not straightforward and, indeed, composite fans that involve more than one of these transport processes may be the rule rather than the exception. Alluvial fans investigated in the Jotunheimen and SE Jostedalsbreen regions of southern Norway (Lewis and Birnie 2001; McEwen et al.

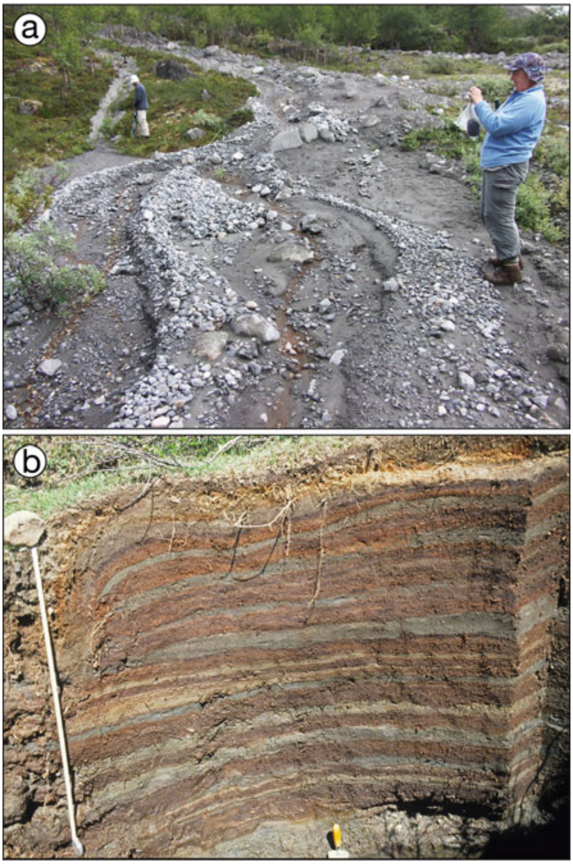

Fig. 7 **a** Modern debris-flow in Leirdalen, Jotunheimen. **b** Distal debris-flow sediments (*grey*) between peat layers (*brown*) in a valley-floor mire at Sletthamn, Leirdalen, excavated in 1996

2011, 2020; Matthews et al. 2020b) demonstrate a complex evolutionary history dominated by debris floods.

The subalpine fans in the SE Jostedalsbreen region (Matthews et al. 2020b) are located at 300–400 m a.s.l. and occupy areas of 0.16–0.51 km^2. The steep, rugged catchments are 1.17–3.44 m^2 in area, with a local relief of 1170–1380 m, and their present glacierized areas are between zero and 56%. The lower altitudinal limit of discontinuous permafrost currently lies at ~1600 m in the region (Fig. 2). Schmidt-hammer exposure-age dating applied to 47 distinctive boulder deposits (e.g. Fig. 8a) on the surface of four of the fans yielded ages ranging from 9.5 ± 0.8 to 2.0 ± 0.8 ka, with a peak age-frequency between ~9.0 and 8.0 ka (Fig. 5i). The main phase of fan aggradation occurred shortly after local deglaciation at ~9.7 ka. A secondary phase of renewed aggradation followed increasing glacierization of the catchments (Neoglaciation) after ~4.0 ka. The Holocene chronology of debris-flood events (Fig. 5i) differs appreciably from those of debris flows (Figs. 5g, h, l) and river floods (Figs. 5e, f).

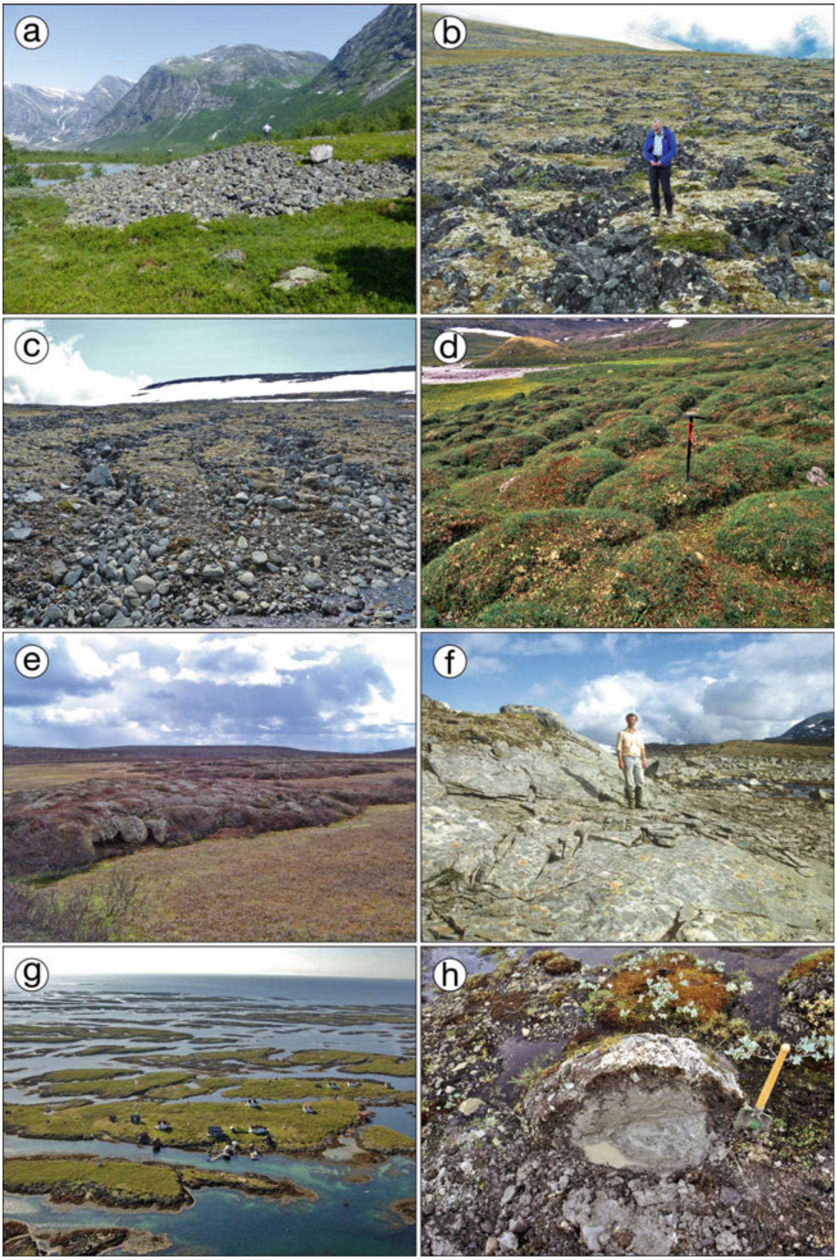
a
b
c
d
e
f
g
h

◀**Fig. 8** Selected periglacial landforms in Scandinavia (*continued*). **a** Debris-flood boulder deposits on the Kupegjellet alluvial fan, SE Jostedalsbreen southern Norway (photo: Geraint Owen). **b** Sorted circles, Juvflye, Jotunheimen (photo: Jennifer Hill). **c** Sorted stripes, Juvflye, Jotunheimen (photo: Jennifer Hill). **d** Earth hummocks, Breidsæterdalen, Jotunheimen (photo; Stefan Winkler). **e** Palsa, Vaisjaggi, Utsjoki, northern Finland (photo: Olli Ruth). **f** Lacustrine rock platform, Bøverbrevatnet, Sognefjell, southern Norway (photo: John Matthews). **g** Strandflat, Helgeland coast, northern Norway (photo: www.visithelgeland.no); **h** boulder-cored frost boil, Styggedalsbreen glacier foreland, Jotunheimen (photo: Stefan Winkler)

The main aggradational phase on fans in the SE Jostedalsbreen region is attributed to debris floods (debris torrents or hyperconcentrated flows), which form a distinct flow type (intermediate between water flows and debris flows) characterised by debris concentrations of 40–70% by weight (cf. Costa 1984; Slaymaker 1988; Wilford et al. 2004; Pierson 2005; Ouellet and Germain 2014; De Haas et al. 2015; Heisser et al. 2015). Such high debris concentrations are explicable in terms of paraglacial conditions in the early Holocene, when till deposits on the extremely steep and unvegetated slopes of the catchments would have been first exposed to subaerial processes (cf. Curry 2000). Rainstorms, snow meltwater, melting glacier ice, thawing permafrost and/or thawing ground exposed from beneath cold-based glacier ice, in combination with the available sedimentary material, would have provided optimal environmental conditions for debris-flood generation. Such optimal conditions would have been attained with decreasing frequency through the mid Holocene and were never attained again, even during Neoglaciation in the late Holocene. By this time, available regolith on the upper slopes of the catchment is likely to have been reduced, if not exhausted, and tree cover would have extended over much of the lower catchment, adding to the stability of possible sediment sources there.

3.2.9 Slope Wash

Colluvial sand layers, typically of thickness 1–10 cm, separated by 1–5 cm thick charcoal layers in the bottom of seven kettle holes in an esker landscape at Kuttanen, Finnish Lapland, enabled Matthews and Seppälä (2015) to establish a unique Holocene chronology of slope-wash events (Fig. 5m).

Several qualities of these kettle holes enabled this reconstruction. First, the enclosed hollows provide efficient traps for sediment eroded from the slopes. Second, the well-sorted sand substrate is highly erodible. Third, the steepness of the side slopes of the kettle holes (maximum slope angles of up to 26° today) enabled slope-wash processes to operate throughout the Holocene. Fourth, the surrounding stands of fire-prone Scots pine (*Pinus sylvestris*) mixed with mountain birch (*Betula pubescens*) provided a source of charcoal for radiocarbon dating. Fifth, the microclimate in the kettle holes (cf. Rikkinen 1989; Tikkanen and Heikkila 1991) allowed cold-air drainage, frost damage and snow drifting to prevent the growth of trees on the lower slopes, enhancing instability on the slopes, and preserving the colluvial stratigraphy at the base.

Radiocarbon dating of 131 charcoal samples established the timing of forest fires that triggered colluvial events by destroying the vegetation cover, as first proposed by Seppälä (1981). Recovery of the forest then provided the fuel for the next fire, followed by re-activation of colluvial processes. Around 50 individual forest fires/colluvial events were identified by Matthews and Seppälä (2015), which represents an average fire frequency of 1 in ~200 years during the Holocene. The frequency of events increased rapidly between ~9.0 and 8.0 ka, attained its peak in the Holocene Thermal Maximum (when the pine forest reached its maximum density), and declined after ~4.0 ka (Fig. 5m). Thus, peak forest fire frequency and colluvial activity appear to have been associated with the warmest weather of the Holocene with its attendant droughts, convective storms and lightning strikes.

3.3 Low-Gradient Landscapes: Inland and Coastal

Where slope failure and rapid mass movement no longer dominate geomorphological activity in the landscape, a different set of processes and landforms becomes apparent. On low gradients, cryoturbation processes, such as frost heave, frost sorting, frost creep and gelifluction, take on a leading role. Characteristic landforms include, amongst others, patterned ground, solifluction lobes, permafrost mounds and stone pavements. In Scandinavia, these landforms and processes occur in the alpine zones with permafrost and seasonal frost, on plateau surfaces, in peatlands and dunefields, and along lacustrine and coastal shorelines.

3.3.1 Sorted Patterned Ground

Repeated freezing and thawing of regolith results in regular patterns at the ground surface, manifest either in terms of coarse and fine sediment (sorted patterned ground) or small-scale topographic variation (unsorted patterned ground). The difference between the two largely reflects whether the sediment involved is a diamicton that contains clasts in a fine, frost-susceptible matrix, or consists of fine sediment alone (Ballantyne 2018). On horizontal or near-horizontal land surfaces, circles and nets result from differential frost heave. Sorted forms are produced in response to the vertical and lateral frost sorting of different clast sizes within diamictons. Where the surface gradient exceeds a few degrees, circles are transformed by gelifluction into stripes.

Large-scale sorted circles (Fig. 8b) and sorted stripes (Fig. 8c) occur extensively in Scandinavia on the flattest parts of the high plateaux, commonly within the blockfield areas discussed previously. Although they are widespread within the permafrost zone, they do not appear to require permafrost for their formation, only a sufficiently deep active layer (Ballantyne 2018). Excellent examples have been described, mapped and analysed from the Juvflye plateau (Galdhøpiggen massif, Jotunheimen), on till surfaces within the permafrost zone at an altitude of ~1750–1950 m a.s.l., where sorted circles predominate on gradients of 0–3°, average of 2°, and sorted stripes on gradients of 3–17°, with an average of 7° (Ødegård et al. 1987, 1988; Winkler et al. 2021). Sorted patterned ground occupies 20–50% of the Juvflye plateau by area. Typically, the fine centres of circles have diameters of 3.0–5.0 m, which is also the average spacing between coarse stripes. At altitudes of >1950 m a.s.l., in areas dominated by in situ frost weathered regolith, they are typically smaller with diameters of 0.5–1.5 m (Ødegård et al. 1988).

Schmidt-hammer exposure-age dating of boulders in the coarse gutters of both sorted circles and sorted stripes at Juvflye (Winkler et al. 2016, 2020) indicate structural stability, at least since the early Holocene. Dates from sorted circles ranged from 8.2 ± 0.5 to 6.9 ± 0.5 ka (Winkler et al. 2016) and exhibited a significant decrease in age with increasing altitude between 1500 and 1950 m a.s.l. The age range from sorted stripes was similar, 8.0 ± 0.4 to 6.7 ± 0.4 ka (Winkler et al. 2020), but with little or no relationship to altitude. Areas of fine sediment between the coarse gutters commonly exhibit evidence of cryoturbation today, especially at relatively high-altitude sites, but this does not affect the boulders that are wedged together in the gutters. Cessation of major activity correlates with the onset of the Holocene Thermal Maximum at ~8.0 ka, declining moisture availability, and a rise in the lower altitudinal limit of discontinuous permafrost to ~1650–1700 m a.s.l. (Lilleøren et al. 2012) but there are several possible mechanistic explanations for the timing of stabilisation. Winkler et al. (2016) proposed three: (1) changes to moisture conditions and related thermodynamics in the active layer affecting frost sorting; (2) loss of fines and reduced frost susceptibility in the gutters; and (3) exhaustion of the supply of boulders from the fines-dominated areas.

The timing of the initiation of sorted patterned ground formation is more problematic. Although some areas of sorted patterned ground could have survived beneath cold-based ice sheets and could be as old as some blockfields (cf. Kleman et al. 2008; Andersen et al. 2019) others, including those at Juvflye, have formed in till and appear to have evolved over a relatively short period in deep, water-saturated active layers following deglaciation in the early Holocene. Rapid development of sorted circles on the Little Ice Age glacier foreland of Slettmarksbreen (Ballantyne and Matthews 1982) and their occurrence on ice-cored moraines at Gråsubreen (Matthews et al. 2014; Winkler et al. 2021), both in Jotunheimen, may provide modern analogues of this process. At Slettmarksbreen, sorted circles up to 3.5 m in diameter formed and stabilised within 50 years of glacier retreat from the site. There, rapid development occurred in water-saturated till immediately after deglacierisation, and stabilisation (indicated by vegetation development on the fine centres and lichen growth on boulders in the gutters) followed shortly after that.

In summary, therefore, we suggest that much of the large sorted patterned ground located in the present permafrost zone of Scandinavia evolved in the early Holocene (sometimes in older regolith of periglacial or glacial origin), is essentially relict, and may not have required permafrost for its formation.

3.3.2 Non-sorted Patterned Ground

Non-sorted patterned ground has been less intensively studied in Scandinavia than the sorted variety. Three types are considered here: (1) frost-crack polygons and sand-wedge polygons in areas of seasonal frost; (2) relict large-scale frost polygons, which traditionally were associated with thermal cracking and ice-wedge growth in formerly more extensive permafrost zones; and (3) active earth hummocks (thúfur) and peaty earth hummocks (pounus). Frost cracks, frost-crack polygons and sand-wedge polygons have been reported from northern Norway to southern Sweden (Svensson 1969; Aartolahti 1972; Seppälä 1982, 2004). Indeed, Svensson (1974) observed modern ground cracking in southern Sweden following the passage of extremely cold air. In the Hietatievat dunefield in northern Finland, Seppälä (1982, 2004) described irregular frost-crack polygons with sides 1–12 m in length, central open cracks 5–15 cm deep, and sand wedges <70 cm deep. The wedges form where the groundwater table is close to the surface in a deflation basin where the mean annual air temperature is –1.5 °C but the winter air temperature often drops to –40 °C.

Svensson (1964, 1988) recognised three lowland areas in Scandinavia with ice-wedge casts forming polygonal patterns: southwestern Jutland, Denmark (outside the limit of the Last Glacial Maximum shown in Fig. 1), Scania, southwestern Sweden, and the Varanger Peninsula, northern Norway (both outside the limit of the Younger Dryas Ice Sheet). Kolstrup (2004) investigated a site in Jutland (Tjæreborg) and assigned Saalian or early-Weichselian ages on the basis of thermoluminescence dates on both wedge infill and host sediments. Her dates ranged from 290 ± 20 to 133 ± 12 ka. In northern Norway, locations on raised shorelines of known age suggest ice wedges were last active under permafrost conditions during the Younger Dryas (see also Sollid et al. 1973). Early descriptions of similar forms inside the limit of the Younger Dryas Ice Sheet on valley floors in northern Sweden, where diameters of 10 to 40 m have been reported (Lundqvist 1964; Rapp and Clark 1971; Rapp 1982), are consistent with their survival beneath cold-based ice according to the 'Kleman model' (Kleman et al. 2008). Even in the areas of continuous permafrost, it appears that modern climatic conditions in Scandinavia have not been suitable for repeated thermal cracking, frost-wedge growth and active frost-polygon development, but this requires further investigation.

Earth hummocks (thúfur) are vegetated, dome-shaped mounds (Fig.8d), typically 0.5 m high and 1.0 m basal diameter, separated by troughs that are generally narrower than the mounds, and composed predominantly of minerogenic sediment (Schunke and Zoltai 1988; Grab 2005). In Scandinavia, they are active today in the low alpine zone throughout the Scandes (e.g. Lundqvist 1964). In northern Finland, similar peaty earth hummocks (pounus) are composed wholly or partly of peat with a minerogenic core and commonly contain permafrost (Luoto and Seppälä 2002a; Van Vliet-Lanoë and Seppälä 2002). Hummocks require moist, moderately well-drained sites to promote frost heave (Van Vliet Lanoë et al. 1993), while vegetation growing on mineral soil or peat has a role in preserving the mound shape. Examples of both types of hummocks have been dated with radiocarbon, and results have been interpreted as indicative of the onset of hummock development. Ellis (1983) obtained seven radiocarbon dates from two hummocks in Jotunheimen, southern Norway, which yielded ages of 4800 ± 220 to 3050 ± 80 cal year BP, whereas 11 ages obtained by Van Vliet-Lanoë and Seppälä (2002) from six pounus in Finnish Lapland were mostly <2.0 ka but ranging from modern to 4050 ± 140 (all dates ± 2σ). Both sites suggest that hummock formation began during late-Holocene climatic deterioration and that hummocks are active at present.

3.3.3 Solifluction Landforms

Solifluction lobes and sheets/terraces are equally if not more common than earth hummocks in the Scandinavian alpine zone, where they occur over a wide range of altitudes on permafrost and non-permafrost slopes (Lundqvist 1964; Williams 1957; Rudberg 1977; Ridefelt and Boelhouwers 2006; Harris et al. 2008; Hjort 2014). They are produced by the slow downslope flow of water-saturated regolith, mainly due to thaw consolidation of ice-rich sediments (gelifluction) and where flow is retarded by vegetation (turf-banked forms) and/or boulder accumulations (stone-banked forms). Alpine vegetation is particularly important in stabilising and maintaining the distinct shape of the step-like riser and tread components of the landform (Eichel et al. 2017), and contribute to the abundance and size of turf-banked solifluction lobes at relatively low altitudes in the zone of seasonal frost (Ulfstedt 1993; Ridefelt and Boelhouwers 2006). Tread dimensions are variable but risers are typically 0.5–1.0 m high and advance downslope at typical rates of 1.0–10.0 mm per year (Ridefelt et al. 2009; Ballantyne 2018). Ploughing blocks, which move downslope at faster rates than the surrounding material, are commonly found in areas of solifluction and are attributed to the thermal properties and weight of the block interacting with thaw consolidation processes. First recognised in Scandinavia by Sernander (1905), the largest known reported example with dimensions 4.9 × 5.0 × 5.6 m and an estimated weight of 36,400 kg, has a 42.5 m linear depression in its wake (Reid and Nesje 1988).

Frontal advance of solifluction lobes and concomitant burial of radiocarbon datable organic soil material have provided an approach to understanding the evolution of solifluction lobes, changing rates of solifluction, and relationships to Holocene climate. Scandinavian studies of this type have been attempted in northern Norway (Worsley and Harris 1974; Ellis 1979; Elliott and Worsley 1999, 2012), southern Norway (Matthews et al. 1986a; Nesje 1993; Nesje et al. 1989), northern Sweden (Rapp and Åkerman 1993) and Finnish Lapland (Kejonen 1979; Matthews et al. 2005). The general conclusion from these studies is that widespread solifluction lobe development occurred after the Holocene Thermal Maximum, between ~5.0 and 3.0 ka, and has continued until modern times with variations in rate. However, there are problems with this approach of which the apparent mean residence time of soil humus and the potential for erosion of the buried soil surface are of particular importance as they can lead to overestimates of time elapsed since burial by hundreds, if not thousands, of years (Matthews 1985, 1993).

Matthews et al. (2005) were able to overcome these two main potential errors by dating soil charcoal rather than soil humus, which was possible because of the special microclimate of their study site at Pippokangas in a 15-m deep kettle hole surrounded by mixed pine and birch forest. Stacked solifluction lobes with risers and treads up to 40 cm high and 8 m long occur on the <10° lower slopes of the kettle hole, where tree growth is prevented by frost damage and the accumulation of snow, as discussed above in relation to slope wash (cf. Rikkinen 1989; Tikkanen and Heikkila 1991). The Pippokangas study involved 46 radiocarbon dates from five solifluction lobes and identified phases of solifluction lobe inception at ~7.4–6.7, 4.2–3.4, 2.6–2.1 and 1.5–0.5 ka (Fig. 5n), which were attributed primarily to millennial-scale variations in effective moisture. However, solifluction activity has been continuous at the site since ~7.0 ka, and monitoring of solifluction rates in northern Sweden has revealed considerable complexity in relationships between solifluction and several climatic variables. Snow depth and both summer and winter temperatures seem to be effective via their influence on active-layer thickness (Åkerman and Johansson 2008; Ridefelt et al. 2009; Strand et al. 2020; see 'The future' below).

3.3.4 Palsas and Lithalsas

According to the classic Scandinavian definition, palsas (Fig. 8e) are peat-covered, dome-shaped perennial permafrost mounds up to 10 m high, which rise out of mires in discontinuous or sporadic permafrost zones (Seppälä 1986, 2011). However, their form may deviate considerably from a dome and include lower, irregular forms (so-called 'palsa plateaux') that have diameters of hundreds of metres (Sannel, 2020). Palsas may also be seen as one end of a continuum of landforms, from mounds formed wholly of peat, through peat-covered mounds with a mineral core, to lithalsas, which are mounds composed wholly of mineral sediments (Åhman 1976, 1977; Gurney 2001; Pissart 2002, 2013). Seppälä (1994, 1995b) demonstrated experimentally that the permafrost core of a palsa grows in areas of the mire where a shallow snow depth allows relatively deep frost penetration in winter. The palsa then survives the summer thaw because of the insulating properties of the peat cover. Palsas formed wholly of peat are uncommon and relatively small, whereas palsas with a mineral core grow larger because the frost susceptibility of the mineral substrate is much greater than that of the peat, promoting the development of ice lenses within the mound. Beyond the distribution of peatlands, lithalsas require cooler summers for preservation of the permafrost core and therefore tend to occur at higher altitudes and/or latitudes than palsas.

Palsas and lithalsas commonly occur in groups within which mounds of varying size represent different stages of development and decay, which is indicative of 'cyclic' development (Seppälä 1988; Matthews et al. 1997b). Permafrost degradation follows the growth of the mound, erosion of surface material, and exposure of the permafrost core to the atmosphere. This leads to thermokarst pools, of which those formed from lithalsas are more likely to be surrounded by rim-ridge ramparts and to survive as relicts in the landscape (Luoto and Seppälä 2002b, 2003).

The radiocarbon dating of palsas has been based on the ability to recognise changing ecological conditions on the mound as it emerges from the mire; specifically the transition from hygrophilous to xerophilous peat as indicated by pollen and macrofossil content. Although early attempts revealed dates from the frozen core in stratigraphic order, problems such as the removal of surface peat by deflation, and cyclic development were not sufficiently appreciated (Seppälä 2003, 2005a, b). In summarizing the dates obtained by Vorren and Vorren (1975), Vorren (1979) and others, Seppälä (1988, 2005a, b) thought that the palsas of Scandinavia are no older than ~3.0 ka and that most formed after 1.0 ka, some under the modern climatic regime. More recent research by Oksanen (2005, 2006) concluded that permafrost aggradation in the palsa mires of northern Finland and northern Pechoria (Russia) began no later than 2.5 and 3.0 ka, and possibly as early as ~4.0 and 5.0 ka, respectively.

3.3.5 Rivers, Lakes and Groundwater

Periglacial rivers, lakes and groundwater are influenced by distinctive hydrological regimes and processes linked to the presence of snow and ice in catchments, in channels and along shorelines (Beldring et al. 2008; Beylich and Laute 2021). Ice jams, flooding and erosion during the break-up of river ice (Lind et al. 2014), ice-push landforms around lakes (Alestalo and Häikiö 1979; Alestalo 1980; Worsley 2008), slushflows (Nyberg 1985, 1989; Clark and Seppälä 1988) and icings (naled or aufeis), and frost weathering associated with inland water bodies (Matthews et al. 1986b; Shakesby and Matthews 1987; McEwen and Matthews 1998; McEwen et al. 2002; Aarseth and Fosen, 2004a, b), are amongst the periglacial landforms and processes that have been described in Scandinavia.

Frost weathering of bedrock in the context of both river channels and lake shorelines provides insights into how effective this process can be in those places within periglacial landscapes where there is sufficient available water. In relation to four gorges on the Storutla, Jotunheimen, McEwen et al. (2002) estimated that frost weathering accounted for excavation of a minimum of 24–97% of gorge volume during the Holocene, at incision rates of 0.15–0.39 mm per year. These values for periglaciofluvial erosion of bedrock appear to exceed those of temperate fluvial systems unaffected by tectonic uplift. Deep penetration of seasonal frost into bedrock channel walls occurs in winter when water levels are low but there is still unfrozen water beneath river ice, especially in areas of the channel floor with relatively deep pools of water. Unfrozen water is drawn to the freezing front, enabling the growth of ice within cracks and inducing the frost weathering of bedrock close to the winter water level in the gorge. This model, which focuses on the annual freeze-thaw cycle, was first developed by Matthews et al. (1986b) to explain the rapid development of rock platforms around a short-lived moraine-dammed lake in Jotunheimen. During the existence of Bøverbrevatnet for between 75 and 125 years, platforms up to 5.3 m wide with backing cliffs up to 1.55 m high were produced (Fig. 8f). No other mechanism than frost weathering is capable of producing platforms in lacustrine environments where wave erosion is extremely limited and lake-ice activity is hardly capable of moving the large, angular (frost-shattered) blocks that remain largely in place as a fringing boulder pavement.

There are major questions about the importance of the fluvial component of denudation in periglacial landscapes where the traditional assumption was that frost weathering and mass movement processes dominate. The classical sediment budget approach developed in the Kärkevagge valley, northern Sweden (Rapp 1960) was instrumental in correcting this assumption. His monitoring of several different components of denudation showed that the solutional load of rivers (and hence chemical weathering) was the dominant process. Scaling-up such results is, however, difficult and later research has demonstrated the differences that exist within Scandinavian periglacial landscapes.

Dissolved load, suspended load and bedload have since been monitored in several catchments in northern (Latnjavagge, Swedish Lappland), middle (Homla, Trøndelag) and southern Scandinavia (Erdalen and Bødalen, western Norway (Beylich 2011; Beylich et al. 2004, 2005; Beylich and Laute 2012, 2018, 2021). This research has, in the main, corroborated Rapp's conclusions. In the partly glacierized western Norwegian oceanic catchments total fluvial denudation is 1.6–3 times that in the non-glacierized Homla catchment, where chemical denudation accounts for 77% of the total fluvial denudation, and is 3.4 times that of mechanical fluvial denudation (i.e. the sum of that attributed to suspended and bedload components combined). Corrected for atmospheric chemical inputs, the mean annual chemical denudation rate for the Homla catchment is 12.1 t km^{-2} a^{-1}, whereas the mean annual suspended sediment yield is 3.3 t km^{-2} a^{-1} and the mean annual bedload yield is 0.3 t km^{-2} a^{-1} (Beylich 2021). Comparative chemical denudation rates estimated for Kärkevagge (Darmody et al. 2000) and the neighbouring Latnjavagge (Beylich 2011) are 19.2 t km^{-2} a^{-1} and 4.9 t km^{-2} a^{-1}, respectively.

Most of the chemical load of rivers originates via groundwater from the regolith and reflects the effectiveness of chemical weathering in both sediments and soils (Darmody and Thorn 1997; Darmody et al. 2000; Thorn et al. 2007, 2011). Studies of differential weathering of minerals exposed to the atmosphere on glacially-scoured bedrock outcrops shed light on the effectiveness and rate of chemical weathering of bedrock throughout Scandinavian periglacial landscapes (André 2002; Nicholson, 2008, 2009; Owen et al. 2007; Matthews and Owen 2011). Based mainly on the negligible weathering of protruding quartzitic veins, average rates of rock-surface lowering at these Scandinavian periglacial sites appear to range from 0.2 to 4.8 mm per thousand years for resistant metamorphic lithologies. However, such estimates may also include the effects of granular disintegration by frost and biological weathering (McCarroll 1990; McCarroll and Viles 1995; Matthews and Owen 2011). On calcareous lithologies, which are not common in Scandinavia, rates of rock-surface lowering may be much higher, especially in hydrologically favourable localities, such as lake shorelines (Owen et al. 2006b).

3.3.6 Inland Aeolian Dunefields and loess

Wind is an important and somewhat neglected geomorphic agent of erosion, transport and deposition in periglacial landscapes. Open spaces and sparse vegetation in cold climates permit aeolian processes to act on the landscape both directly through abrasion, sand drift and deflation, and indirectly through snow-drift and frost-action effects (Seppälä 2004), to which must be added their role in drifting lake ice and, at the coast, sea ice (e.g. Alestalo and Häikiö 1975).

Erosive effects of wind abrasion in the form of ventifacts (faceted and grooved boulders) and polished boulders in southern Sweden and Denmark have been long recognised as indicators of wind blasting under former periglacial conditions (Milthers 1907; Svensson 1983; Schlyter 1995; Christiansen and Svensson 1998). The distribution and orientation of in situ wind-blasted rock surfaces in relation to ice-sheet limits, combined with associated luminescence dates, leads to the conclusion that formation was associated with easterly winds, mainly at or close to the Last (Weichselian) Glacial Maximum and during subsequent deglaciation. At these times, most probably in the period from 22 to 17 ka, strong easterly katabatic and zonal winds would have dominated in open, sparsely-vegetated landscapes (Christiansen and Svensson 1998).

Largely relict aeolian dunefields comprise a major element of the periglacial landscape across northern Scandinavia (Högbom 1923; Klemsdal 1969; Seppälä 1971, 1972; 1995a; Sollid et al. 1973; Matthews and Seppälä 2014). Luminescence dates up to 10.7 ± 1.2 ka (Kotilainen 2004) establish that mainly parabolic dunes, the arms of which are up to ~1500 m long, ~150 m wide and ~12 m high (Seppälä 1971) formed from the sand blown from eskers, valley trains and other glacigenic deposits shortly after retreat of the Younger Dryas Ice Sheet. The parabolic form of the dunes is the result of the arms being partly anchored by vegetation during their formation, and well-developed, undisturbed stratification (i.e. no niveo-aeolian features) within these dunes indicates that deposition occurred without snow in the summer months (Seppälä 2004).

The subsequent history of many inland dunefields has been investigated in some detail in northern Finland based on dune stratigraphy and the radiocarbon dating of buried palaeopodzols and charcoal layers (Seppälä 1995a, b; Käyhkö et al. 1999; Kotilainen 2004; Matthews and Seppälä 2014). In favourable sites for vegetation growth, initial stabilisation of the parabolic dunes probably occurred within a few hundred years of deglaciation (~10.9–10.2 ka) but at other sites dunes may have remained active for up to 2000 years. Based on analysis of a total of 137 radiocarbon dates on buried charcoal layers from dunes within the northern boreal forest ecotone (the subzone characterised as birch forest with pine stands at present), Matthews and Seppälä (2014) recognised at least 16 dune re-activation events (episodes of deflation) of more than local significance since ~8.3 ka. The available data indicate that dune re-activation was triggered by forest fires, which occurred throughout the Holocene but with increasing frequency in the late Holocene. They proposed a conceptual model summarising the complex geo-ecological interactions between climate and aeolian activity (deflation or stabilisation) modulated by the effects of fire and vegetation on fuel supply and successional recovery. The millennial-scale increase in deflation activity during the late Holocene (Fig. 5o) was attributed to relatively cool and moist climatic conditions, which increased the density of the tree cover in dune habitats and fuelled the fires, while centennial-scale successional recovery of the vegetation cover controlled the recurrence interval to the next fire.

A complementary approach to analysing the relationship between aeolian activity and Holocene climatic variation was adopted by Nielsen et al. (2016a, b), who analysed the input of sand grains to lacustrine sediments at two sites on Lofoten and Andøya on the west coast of northern Norway. At Latjønna, on Andøya (14.5 m a.s.l.), a record of the influx of medium to coarse sand (>250 μm) from 6.0 ka revealed a fluctuating increase in aeolian activity, which reached a distinct maximum at 1.7–0.7 ka. Nielsen et al. (2016b) considered falling sea level made sand available for deflation, and that increasing storminess was the main driver for increased niveo-aeolian transport of sand grains inland during winter. At Trehynnvatnet on Langøya (33 m a.s.l.) the longer record from 11.5 ka (Fig. 5p) showed generally low influx of sand before ~2.8 ka, after which the largest of several activity peaks occurred during the last 0.5 ka. Again, sand transport over snow by southwesterly winds during winter storms was invoked as the preferred process.

Aeolian silt deposits (loess) have seldom been reported from Scandinavia. However, Stevens et al. (2022) have confirmed that thin loess deposits occur at scattered locatities on relatively high ground in central and southern Sweden. Luminescence dating has here yielded mainly early- to mid-Holocene ages, which reflect early-Holocene origins from glacio-fluvial sediments followed by later sediment mixing during soil development and/or redeposition during later phases of landscape instability.

3.3.7 Coastal Rock Platforms and the Strandflat

Frost weathering has been proposed as the primary agent of cliff recession and platform extension in areas of restricted fetch within fjords along the coast of northern Norway for over a century. Vogt (1918) described rock platforms up to 12 m wide, close to high-tide level in Kvænangen fjord, on which angular fragmented bedrock showed little or no evidence of rounding by wave action. The Norwegian explorer, scientist and diplomat, Fridtjof Nansen described similar rock platforms up to 20 m wide close to his house on the Fornebo peninsula in inner Oslo fjord (Nansen 1922). More recently, Sollid et al. (1973) reported that the inner edge of 49 present-day coastal rock platforms in Finnmark occur at 1.4 ± 0.6 m above mean tide level, while 12 present-day coastal rock platforms on Hinnöya (Lofoten Islands) occur at 1.5 ± 0.5 m above mean tide level (Möller and Sollid 1972). At all these fjord locations, platform erosion depends on frost weathering at the cliff base associated with the winter formation of thick layers of shore-fast sea ice, possibly enhanced by brackish water in the fjords, fresh groundwater seepage from the cliffs, ice-foot development, and the subsequent removal of weathered material by storm waves and/or ice-rafting.

Frost weathering has been important also in the formation of relict rock platforms, which have been raised above present sea level by glacio-isostatic land uplift. This is particularly clear in the case of the main Younger Dryas shoreline in northern Norway, which is best developed in narrow fjords and sounds, but is absent from wave-exposed headlands (Andersen 1968; Sollid et al. 1973; Rasmussen 1981; Blikra and Longva 1985), and was eroded when a permafrost climatic regime existed down to sea level. Precise mechanisms of weathering and erosional processes associated with both active and relict coastal rock platforms are, however, poorly understood. Despite the moderating effect of saltwater, and a greater role for wave action at coastal locations, frost weathering on lake shores (e.g. Fig. 8f), as discussed above, may provide a model for the rapid formation of coastal rock platforms in periglacial environments (Matthews et al. 1986b; Dawson et al. 1987). Further investigations on modern periglacial coasts, such as that of Ødegård and Sollid (1993) in Svalbard, are required to clarify the disputed nature and effectiveness of the processes involved in cold-climate rock-platform erosion (cf. Dawson 1979; Byrne and Dionne 2002; Hansom et al. 2014).

On much longer timescales, frost weathering is one of the main processes responsible for the Norwegian strandflat (Fig. 8g). This is a horizontal to gently sloping, uneven bedrock coastal plain or foreland, with numerous low islands, skerries and submarine and subaerial rock platforms (Corner 2005b). The strandflat is present along much of the Norwegian coast but is regionally variable in extent and elevation: it is up to 60 km wide and ranges from 40 m below sea level to a maximum of 100 m a.s.l. After a long debate and many different theories concerning its age and origin (e.g. Reusch 1894; Nansen 1922; Klemsdal 1982; Larsen and Holtedahl 1985; Guilcher et al. 1986; Holtedahl 1998; Olesen et al. 2013; Fredin et al. 2017), the emerging picture is of a polygenetic landform that has evolved since pre-Quaternary times.

The latest major formative events involved processes of frost weathering, sea-ice erosion and wave abrasion, modified by glacial erosion, essentially as proposed by Nansen (1922). These events are encompassed by the theory, proposed by Porter (1989) that the age of the strandflat is primarily accounted for by average glacial conditions during the early Pleistocene (~2.6–0.9 Ma). During that interval, ice sheets were smaller than in the late Quaternary (cf. Kleman et al. 2008) and, crucially, would not have reached a coastal zone exposed to frost weathering during moderately low relative sea levels. Meanwhile, variable glacier extents and glacio-isostatic and glacio-eustatic changes in sea level would have affected the wide range of elevations and gradients exhibited by the strandflat today.

3.4 Glacier-Foreland Landscapes

Glacier forelands—the landscapes deglacierised since the Little Ice Age glacier maximum of the last few centuries, and continuing to be deglacierised today—provide an opportunity to investigate a range of periglacial landforms and processes.

The main advantage of these landscapes is that they can be viewed as microcosms or field laboratories, without the long and complex evolutionary history of the plateau, steepland and low-gradient landscapes already discussed. Furthermore, the short timescale for landform development can often be firmly established by invoking the chronosequence concept (cf. Matthews 1992; Ballantyne 2002; Heckmann and Morche 2019). In Scandinavia, several studies of this nature have provided insights into active (neo)paraglacial and periglacial processes following glacier retreat under present climatic regimes. In some cases, such studies may provide modern analogues for interpreting relict landforms, as already indicated in relation to the formation of frost-sorted patterned ground (*sorted circles*) and frost-weathered shorelines (*rock platforms*). Further selected examples are considered here.

Glacier retreat from steep Little Ice Age lateral moraines, and the ensuing modification of slope form by gully erosion and debris-flow activity, have been investigated in detail at Fåberstølsbreen and other outlet glaciers of the Jostedalsbreen ice cap (Ballantyne and Benn 1994, 1996; Ballantyne 1995; Curry and Ballantyne 1999; Curry 1999, 2000). Such neoparaglacial activity is initiated by rainstorms and snow meltwater. The main agent of erosion and sediment transport is debris flow with a minor role for snow avalanches, and colluvial fans are deposited at the foot of the moraine slope. Ballantyne and Benn (1994) recorded ~10 debris flows per year over a six-year observation period at Fåberstølsbreen. At this glacier foreland, and at neighbouring Bergsetbreen, Ballantyne (1995) showed that a stable neoparaglacial landsystem is produced within centuries, if not decades of deglaciation. This landsystem consists of gully-head areas eroded to bedrock, broad intersecting gullies in mid-slope position, coalescing debris-flow fans at the slope foot, and valley-floor deposits.

A small but perfectly formed rock glacier that developed from the outermost Little Ice Age lateral moraine of Bukkeholsbreen, Jotunheimen, exemplifies the rapid development and stabilisation of another steepland landform (Vere and Matthews 1985). The rock glacier is about 160 m long and 130 m wide, with an average surface slope of 10°, and several well-developed arcuate transverse ridges. According to lichenometric dating, it formed and stabilised within ~200 years of moraine deposition ~AD 1750. Formation of a rock glacier in this way indicates the importance of a sufficiently large debris supply, combined with the opportunity for incorporation of buried glacier ice or interstitial ice from overridden distal snowbeds.

On low-gradient parts of Norwegian glacier forelands, the processes of frost heave, frost sorting and slow mass movement (solifluction) are often in evidence. Boulder-cored frost boils (Fig. 8h) produced by the up-heaval of individual boulders in poorly drained areas of till were described by Harris and Matthews (1984) on the glacier forelands of Storbreen and Bøverbreen, Jotunheimen. Ballantyne and Matthews (1983) investigated the steady development of small-scale crack networks (probably desiccation cracks) into sorted polygons <0.5 m in diameter on terrain deglaciated from 0 to 35 years at Storbreen. Similar polygonal forms recognised at Styggedalsbreen by Matthews et al. (1998) and Haugland (2004, 2006), developed and stabilised close to the ice margin after ~60 years, on the flat tops of low, degraded annual moraines. The sorted polygons transitioned to sorted stripes on gradients of 13–17°, on the upper slopes of the degraded moraines. At the same location, Matthews et al. (1998) mapped boulder-cored frost boils, solifluction lobes with risers up to 30 cm high, ploughing blocks, and shallow accumulations of colluvial sand (possible slope wash and/or niveo-aeolian deposits), the sites of which were differentiated by moisture availability, gradient and exposure, as reflected in microtopography. Another study at Storbreen (Matthews and Vater 2015) demonstrated the rapid development of stone pavements within ~25 years of deglacierisation. Pavement formation was attributed to the combined action of pervection (downwashing of fine particles, particularly silt, from the surface layers), frost sorting (the raising of relatively large clasts towards the surface) and deflation (lateral removal of sand-sized particles by wind).

Biogeomorphological and geo-ecological approaches to glacier-foreland landscapes in Jotunheimen have improved understanding of the interaction of organisms with physico-chemical periglacial processes in landform, soil and vegetation development (Matthews 1992). Vegetation succession and soil development on sorted and non-sorted patterned ground signal rapid stabilisation of the landforms (Ballantyne and Matthews 1983; Matthews et al. 1998; Haugland and Beaty 2005; Haugland and Owen 2005; Haugland and Owen-Haugland 2008). Solifluction and ploughing boulders remain active on older terrain, where lobe development is promoted by the binding action of the vegetation cover (Matthews et al. 1998; Matthews 1999). Boulder-cored frost boils (Fig. 8h) also remain active but are unaffected by vegetation. Chemical weathering in sediments and soils is also enhanced as vegetation develops on glacier forelands (Darmody and Thorn 1997; Thorn et al. 2007, 2011); and on recently-deposited boulder surfaces, Matthews and Owen (2008) showed that endolithic lichens may enhance rock weathering rates by up to two orders of magnitude.

4 The Significance of Periglacial Dynamics in Scandinavia within the European context

This review concludes that Scandinavian periglacial landscapes have evolved over a long period of geological time; that only a minority of landforms are in equilibrium with present-day periglacial processes and climates; and that many elements of these landscapes are polygenetic and either relict or continuing to develop under changing Holocene and anthropocene environmental conditions.

4.1 Continual Environmental Change

It is perhaps surprising that so many elements of the periglacial landscapes of Scandinavia are so poorly adjusted to present environmental conditions, despite the widespread occurrence of permafrost and seasonal frost (Fig. 1). This is attributed to a number of factors, including the preservation of relatively old elements beneath cold-based ice sheets during the Pleistocene, paraglacial effects, and continuing environmental change during the Holocene when landforms may vary in their level of activity, become relict or be re-activated.

Possible pre-Quaternary elements are recognisable in the major topographic elements in today's periglacial landscapes, such as the inland plateaux and the coastal strandflat. During the Pleistocene, the cumulative effect of repeated glacial and interglacial episodes also left their mark on the distribution of specific landforms, such as blockfields. However, it is the environmental changes at the end of the Last Glaciation (the Weichselian Lateglacial) and the relatively small variations in climate of the Holocene that account for the active or relict status of many of the landforms and the extent of present activity. Many large rock-slope failures, rock glaciers, pronival ramparts, raised rock platforms and parabolic sand dunes provide examples of landforms that became relict at the Younger Dryas-Holocene transition.

Our survey of the current knowledge of the landforms, their formative processes, and especially their age as determined by the application of dating techniques (particularly radiocarbon dating, luminescance dating, cosmic-ray exposure-age dating and Schmidt-hammer exposure-age dating), has revealed the effectiveness of past environmental change in bringing about geomorphological change. In some cases, the same techniques have reduced our ignorance concerning which landforms and processes are active today and the extent of current activity.

4.2 Landscape as Palimpsest

In many cases it is now possible, using available dating techniques, to place at least approximate ages on relict periglacial landforms, such as blockfields, rock glaciers and sorted patterned ground. However, the allocation of active or relict status is often only a first approximation (cf. Hjort 2006), because recognising the extent of modern activity in the face of environmental change is problematic. Some stratigraphic contexts enable the reconstruction of the changing frequency of events since at least the early Holocene. At certain sites in Scandinavia, this has proved possible using radiocarbon dating; for example, in relation to records of debris flows, snow-avalanches and river floods in southern Norway; and solifluction, slope wash and aeolian activity in northern Finland (Fig. 5). Similarly, exposure-age dating techniques have established Holocene chronologies for coarse-debris deposits, as exemplified by large and small rock-slope failures, snow-avalanche impact ramparts, and debris floods on alluvial fans.

The periglacial landscapes of Scandinavia are therefore complex palimpsests in which active and relict forms exist in close proximity. The term 'palimpsest' has been used before in geomorphology (e.g. Kleman 1992) but not specifically in relation to periglacial landscapes. A palimpsest periglacial landscape is not simply a mosaic of active and relict landforms of specific ages. Although some landforms may be truly relict (formed and stabilised at specific times in the past), many others have more complex histories. Relict forms, such as parabolic dunes may be re-activated. Some may be relict only in part, as in the case of active sorted circles surrounded by relict gutters. Other landforms and processes exhibit varying activity levels and rate changes through time, as exemplified by the Holocene chronologies of Fig. 5.

A final, important implication of the palimpsest concept for understanding periglacial landscapes is the problem it poses for identifying a meaningful altitudinal zonation of landforms in relation to periglacial processes and environmental variables. Past attempts at defining altitudinal zones in Scandinavia, including those of Lundqvist (1964) and Rudberg (1977) in Sweden, Barsch and Treter (1976) and Kergillec (2015) in Rondane, southern Norway, Harris (1982) in Okstindan, northern Norway, Niessen et al. (1992) in northern Finland and, most recently, Winkler et al. (2021) in Jotunheimen, have all encountered this problem, which has yet to be resolved. Altitudinal variation in permafrost limits during the Holocene was of the order of 400 m in southern Scandinavia and 200 m in northern Scandinavia (Lilleøren et al. 2012), which emphasises the scale of the problem. Until active and relict elements of the landscape can be distinguished with confidence there seems little possibility of defining valid or useful altitudinal zonations of the periglacial landscape.

4.3 The Future

There are clear indications that future changes to the periglacial landscapes of Scandinavia are predictable. The dynamic nature of the altitudinal limits of permafrost during the Holocene gives reason to expect greater dynamism in the future. The present extent of permafrost is shrinking in response to current warming trends (Gisnås et al. 2017). Periglacial processes and landforms dependent upon both permafrost and seasonal frost, such as rock weathering, patterned ground, rock glaciers, rock-slope failures and solifluction, will be affected appreciably, if not catastrophically, by the projected future rise in mean annual air temperature (Harris et al. 2009; Aalto et al. 2017; Karjalainen et al. 2020).

The response of periglacial landforms and processes to climate change is, however, complex, as indicated by the following examples from Scandinavia. A good illustration of this complexity is the state of palsas in the sporadic permafrost zone. In northern Finland, small increases in temperature (1 °C) and precipitation (10%) are predicted to lead to considerable losses in areas suitable for palsa development (Fronzek et al. 2006, 2010). These authors tested models that predicted the total disappearance of palsas if mean annual temperature increases by 4 °C. The validity of such predictions is supported by observations and surveys of palsa mires from northern Finland (Luoto and Seppälä 2003) and northern Sweden (Zuidhoff and Kolstrup 2000; Sannel and Kuhry 2011; Sannel et al. 2016; Borge et al. 2017; Olvmo et al. 2020). The degradation of palsas, which can be a response to erosion of the peat cover on top of the aggrading permafrost core and/or melting of the ice core as thermal conditions change and/or increasing summer precipitation, is likely to be most marked near the limits of palsa distribution, as in southern Norway (Sollid and Sørbel 1998). However, local snow condition in particular may permit palsas to survive or new palsas to form even in a warming environment (Seppälä 1994, 2011; Nihlén 2003).

Current thawing of permafrost is also influencing both rapid and slow mass movement. Rock-slope failures tend to be stabilized by permafrost, as shown at the three rockwall sites in southern and northern Norway, where enhanced sliding rates were determined by Hilger et al. (2021) in response to permafrost degradation following the Holocene Thermal Maximum (see above). This implies rock-slope failures may become more frequent during accelerated warming, a suggestion validated by the failure of Veslemannen rockslide (part of the Mannen site investigated by Hilger) on September 5, 2019 (Kristensen et al. 2021). At Veslemannen, five years of monitoring revealed progressive rock-slope weakening as precursor movements, which coincided with precipitation events that increased seasonally from spring to autumn. The seasonal pattern implies thermal control on pore-water pressure, which Kristensen et al. (2021) attribute to the transition from permafrost to seasonal frost. This explanation is supported by thermal monitoring, geophysical surveying and numerical modelling at the Mannen site and the Gámanjunni site in northern Norway (Etzellmüller et al. 2021), and also by the observation by Blikra and Christiansen (2014) of ice-filled fractures at the rockslide site at Nordnesfjell in northern Norway.

Both aerial photography and satellite remote sensing (InSAR) have demonstrated recent velocity acceleration of the rock-glacier complex at Ádjet, northern Norway (Eriksen et al. 2018). Average annual horizontal velocity measured by aerial photography increased from ~0.5 m per year between 1954 and 1977 to ~3.6 m per year between 2006 and 2014. Average annual velocity measurements determined by InSAR increased from ~4.9 to 9.8 m per year between 2009 and 2016, while maximum velocities increased from ~12 to 69 m per year. Results of kinematic analysis are consistent with permafrost degradation and rock-glacier destabilisation following increases in mean annual air temperature of 1.8 °C and annual precipitation of 330 mm (55%) over the 62-year measurement period, leading to increased amounts of water reaching deeper layers within the rock glacier.

Active solifluction has been measured in the Abisko Mountains of northern Sweden (Kärkevagge in the west to Nissunvagge in the east) for over 50 years (Åkerman and Johansson 2008; Ridefelt et al. 2009; Strand et al. 2020). Various methods were used by different research workers to record movement rates. Ridefelt et al. (2009) compiled and analysed the available data in relation to the possible effects of climatic variables. Although variability was high, interpretable regional and temporal patterns were obtained. Generally higher movement rates were found in the western part of the region (Kärkevagge area) characterised by relatively low temperatures but relatively high precipitation and snowfall. Importantly, for data from the Kärkevagge area between 1979 and 2001, an increase in the rate of solifluction movement was detected, and statistically significant positive linear correlations of up to $r = 0.63$ and 0.56 ($p < 0.05$) were established between annual mean movement and annual mean air temperature and autumn (October to December) mean air temperature, respectively. Additional variables found to be significant in multiple regression analyses included summer (July to September) mean air temperature, annual precipitation, winter precipitation, melt start (first day with positive air temperatures) and freeze start (first day with negative air temperatures). The relationships involving freeze start and winter precipitation were negative. Overall, the results reported by Ridefelt et al. (2009) suggest an indirect causal relationship between warming air temperatures and solifluction rates involving an increase in active-layer thickness (affected by summer temperatures) and depth of frost penetration (affected by winter temperatures), moderated by snow depth and meltwater availability.

The complex interactions between periglacial landscapes and climate, some of which have been signalled in the selected examples above, will require a concerted research effort to understand fully likely future climate change impacts. There has already been a major effect on periglacial research agendas and this is likely to continue. In addition, observation, mapping, environmental reconstruction, stratigraphical investigation, dating, monitoring, experimentation, remote sensing, geographical information systems, and modelling, will all need to be embraced with imagination to improve what we already know about periglacial landscapes, past, present and future.

Acknowledgements This chapter is dedicated to Matti Seppälä, who sadly died on 24 November 2020; in appreciation of his immense contribution to periglacial geomorphology in Finland and internationally.

Several colleagues contributed photographs, including Jennifer Hill, Jan Hjort, Richard Mourne, Mons Rustøy, Olli Ruth, Peter Wilson and Stefan Winkler. Pål Ringkjøb Nielsen supplied the data for plotting Fig. 5l. We are also grateful to Ola Fredin, Charles Harris, Miska Luoto, Richard Shakesby, Peter Wilson and Stefan Winkler for reviewing and commenting on the manuscript, and to Anna Ratcliffe who prepared the figures for publication. This paper represents Jotunheimen Research Expeditions, Contribution No. 225 (see http://jotunheimenresearch.wixsite.com/home).

References

Aalto J, Venäläinen A, Heikkinen RK, Luoto M (2014) Potential for extreme loss in high-latitude Earth surface processes due to climate change. Geophys Res Lett 41:3914–3924

Aalto J, Harrison S, Luoto M (2017) Statistical modelling predicts almost complete loss of major periglacial processes in Northern Europe by 2100. Nat Commun 8(1):1–8

Aarseth I, Fosen H (2004a) A Holocene lacustrine platform around Storavatnet, Osterøy, western Norway. Holocene 14:589–596

Aarseth I, Fosen H (2004b) Late Quaternary lacustrine cryoplanation of rock surfaces in and around Bergen, Norway. Norw J Geol 84:125–137

Aartolahti T (1972) Dyynien routahalkeamista ja routahalkeamapolygoneista (English summary: Frost cracks and frost polygons on dunes in Finland). Terra 84:124–131

Alestalo J (1980) Systems of ice movement on Lake Lappajärvi, Finland. Fennia 158:27–39

Alestalo J, Häikiö J (1975) Ice features and ice-thrust shore forms at Luodonselkä, Gulf of Bothnia, in winter 1972/73. Fennia 144:1–24

Åhman R (1976) The structure and morphology of minerogenic palsas in northern Norway. Biul Peryglac 26:25–31

Åhman R (1977) Palsar i Nordnorge. Meddelanden från Lunds Universitets Geografika Institution Avhandlingar 78:1–165
Åkerman HJ, Johansson M (2008) Thawing permafrost and thicker active layers in sub-arctic Sweden. Permafrost Periglac Process 19:279–292
Alestalo J, Häikiö J (1979) Forms created by thermal movement of lake ice in Finland in winter 1972–73. Fennia 157:51–92
Andersen BG (1968) Glcial geology of western Troms, north Norway. Nor Geol Unders 256:1–160
Andersen JL, Egholm DL, Knudsen MF, Linge H, Jansen JD, Pedersen VK, Nielsen SB, Tikhomirov D, Olsen J, Fabel D, Xu S (2018) Widespread erosion on high plateaus during recent glaciations in Scandinavia. Nat Commun 9:830. https://doi.org/10.1028/$41467-018-03280-2
Andersen JL, Egholm DL, Knudsen MF, Linge H, Jansen JD, Goodfellow BW, Pedersen VK, Tikhomirov D, Olsen J, Fredin O (2019) Pleistocene evolution of a Scandinavian plateau landscape. J Geophys Res Earth Surf 123. https://doi.org/10.1029/2018JF004670
Andersson JG (1906) Solifluction: a component of subaerial denudation. J Geol 14:91–112
André MF (2002) Rates of postglacial rock weathering on glacially scoured outcrops (Abisko-Riksgrånsen area, 68° N). Geogr Ann Ser (Phys Geogr) 64:139–150
André M-F (2003) Do periglacial landscapes evolve under periglacial conditions? Geomorphology 52:149–164
André, M-F (2009) From climate to global change geomorphology: contemporary shifts in periglacial geomorphology. In Knight J, Harrison S (eds) Periglacial and paraglacial processes and environments, vol 320. Geological Society, London, Special Publication, pp 5–28
Ballantyne CK (1987) Some observations on the morphology and sedimentology of two active protalus ramparts, Lyngen, northern Norway. Arct Alp Res 19:167–174
Ballantyne CK (1995) Paraglacial debris cone formation on recently deglaciated terrain. Holocene 5:25–33
Ballantyne CK (2002) Paraglacial geomorphology. Quat Sci Rev 21:1935–2017
Ballantyne CK (2010) A general model for autochthonous blockfield evolution. Permafrost Periglac Process 21:289–300
Ballantyne CK (2018) Periglacial geomorphology. Wiley-Blackwell, Chichester
Ballantyne CK, Benn DI (1994) Paraglacial slope adjustment and resedimentation following glacial retreat, Fåbergatølsbreen, Norway. Arct Alp Res 26:255–269
Ballantyne CK, Benn DI (1996) Paraglacial slope adjustment during recent deglaciation and its implications for slope evolution in formerly glaciated environments. In: Anderson MG, Brooks S (eds) Advances in hillslope processes, vol 2. Wiley, Chichester, pp 1173–1195
Ballantyne CK, Matthews JA (1982) The development of sorted circles on recently deglaciated terrain, Jotunheimen, Norway. Arct Alp Res 14:341–354
Ballantyne CK, Matthews JA (1983) Desiccation cracking and sorted polygon development, Jotunheimen, Norway. Arct Alp Res 15:339–349
Barsch D (1971) Rock glaciers and ice-cored moraines. Geogr Ann Ser (Phys Geogr) 53:203–206
Barsch D (1977) Nature and importance of mass wasting by rock glaciers in alpine permafrost environments. Earth Surf Proc Land 2:231–245
Barsch D, Treter U (1976) Zur Verbreitung von Periglazialphänomenen in Rondane/Norwegen. Geogr Ann Ser (Phys Geogr) 58:83–89
Beldring S, Engen-Skaugen T, Førland EJ, Roald LA (2008) Climate change impacts on hydrological processes in Norway based on two methods for transferring regional climate model results to meteorological station sites. Tellus (Dyn Meteorol Ocean) 60(3):439–450
Bellwald B, Hjelstuen BO, Sejrup HP, Stokowy T, Kuvås (2019) Holocene mass movments in west and mid-Norwegian fjords and lakes. Mari Geol 407:192–212
Berthling I, Etzelmüller B (2011) The concept of cryoconditioning in landscape evolution. Quat Res 75:378–384
Berthling I, Shomacker A, Benediktsson ÍÖ (2013) The glacial and periglacial research frontier: where from here? In: Giardino JR, Harbor JM (eds) Treatise on geomorphology, volume 8, glacial and periglacial geomorphology. Academic Press, San Diego, CA, pp 479–498

Beskow G (1935) Tjälbildningen och tjällyftningen med särskild hänsyn till vägar och järnvägar. Sveriges Geologiska Unersökning Avhandlingar och Uppsatser, Arsbok 26, Ser C 375:1–242
Beskow G (1947) Soil freezing and frost heaving with special applications to roads and railroads. Northwestern University Technological Institute: Evanston, IL. [English translation of Beskow (1935) by JO Osterberg.]
Beylich AA (2011) Mass transfers, sediment budgets and relief development in cold environments: results of long-term geomorphologic drainage basin stidies in Iceland, Swedish Lapland and Finnish Lapland. Zeitschrift Für Geomorphologie NF 55:145–174
Beylich AA, Laute K (2012) Spatial variations of surface water chemistry and chemical denudation in the Erdalen drainage basin, Nordfjord, western Norway. Geomorphology 167–168:77–90
Beylich AA, Laute K (2018) Morphoclimatic controls of contemporary chemical and mechanical denudation in a borel-oceanic drainage basin system in central Norway (Homla drainage basin, Trøndelag). Geogr Ann Ser (Phys Geogr) 100:116–139
Beylich AA, Laute K (2021) Fluvial processes and contemporary fluvial denudation in different mountain landscapes in western and central Norway. In: Beylich AA (ed) Landscapes and landforms of Norway. Springer, Berlin, pp 147–168
Beylich AA, Kolstrup E, Thysted T, Gintz D (2004) Water chemistry and its diversity in relation to local factors in the Latnajavagge drainage basin, arctic-oceanic Swedish Lapland. Geomorphology 58:125–143
Beylich AA, Molau U, Luthbom K, Gintz D (2005) Rates of chemical and mechanical fluvial denudation in an arctic-oceanic periglacial environment, Latnajavagge drainage basin, northernmost Swedish Lapland. Arct Antarct Alp Res 37:75–87
Blikra LH, Christiansen HH (2014) A field-based model of permafrost-controlled rockslide deformation in northern Norway. Geomorphology 208:34–49
Blikra LH, Nemec W (1993) Postglacial avalanche activity in western Norway: depositional facies sequences, chronostratigraphy and palaeoclimatic implications. In: Frenzel B, Matthews JA, Gläser B (eds) Soliflucton and climatic variation in the Holocene. Gustav Fischer Verlag, Stuttgart, pp 143–162
Blikra LH, Nemec W (1998) Postglacial colluvium in western Norway: depositional processes, facies and palaeoenvironmental record. Sedimentology 45:909–959
Blikra LH, Nesje A (1997) Holocene avalanche activity in western Norway: chronostratigraphy and palaeoclimatic implications. In Matthews JA, Brunsden D, Frenzel B, Gläser B, Weiß (eds) Rapid mass movement as a source of climatic evidence for the Holocene. Gustav Fischer Verlag: Stuttgart, pp 299–312.
Blikra LH, Hole PA, Rye N (1994) Hurtige Massebevegelser og avsetningstyper i alpiner områder, Indre Nordfjord. Nor Geol Unders Skr 92:1–17
Blikra LH, Selvik SF (1998) Climatic signals recorded in snow avalanche-dominated colluvium in western Norway: depositional facies successions and pollen records. Holocene 8:631–658
Boch SG, Krasnov II (1943) O nagornykh terraskh i drevnikh poverkhnostyakh vyravnivaniya na Urale i svyazannykh s nimi problemakh. Vsesoyuznogo Geograficheskogo obshchestva Izvestiya 75:14–25. [Translated from Russian (1994) On altiplanation terraces and ancient surfaces of levelling in the Urals and associated problems. In Evans DJA (ed) Cold climate landforms. Wiley, Chichester, pp 177–204.]
Bøe AG, Dahl SO, Lie Ø, Nesje A (2006) Holocene river floods in the upper Glomma catchment, southern Norway: high resolution multiproxy record from lacustrine sediments. Holocene 16:445–455
Böhme M, Oppikofer T, Longva O, Jaboyedon M, Hermanns RL, Derron MH (2015) Analyses of past and present rock slope instabilities in a fjord valley: implications for hazard estimations. Geomorphology 248:464–474
Borge AF, Westermann S, Solheim I, Etzelmüller B (2017) Strong degradation of palsas and peat plateaus in northern Norway during the last 60 years. Cryosphere 11:1–16

Byrne M-L, Dionne J-C (2002) Typical aspects of cold regions shorelines. In Hewitt K, Byrne M-L, English M, Young G (eds) Landscapes of transition: landform assemblages and transformations in cold regions. Kluwer, Dordrecht, pp 141–158

Christiansen HH (1998) Nivation forms and processes in unconsolidated sediments, NE Greenland. Earth Surf Proc Land 23:751–760

Christiansen HH, Svensson H (1998) Windpolished boulders as indicators of a Late Weichselian wind regime in Denmark in relation to neighbouring areas. Permafrost Periglac Process 9:1–21

Christiansen HH, Etzelmüller B, Isakssen K, Juliussen H, Farbrot H, Humlum O, Johansson M, Ingeman-Nielsen T, Kristensen L, Hjort J, Holmlund P, Sannel ABK, Sidsgaard C, Åkerman HJ, Foged N, Blikra LH, Pernosky MA, Ødegård RS (2010) The thermal state of permafrost in the Nordic area during the international polar year 2007–2009. Permafrost Periglac Process 21:156–181

Church M, Ryder JM (1972) Paraglacial sedimentation: a consideration of fluvial processes conditioned by glaciation. Geol Soc Am Bull 83:3059–3072

Clark MJ, Seppälä M (1988) Slushflows in a subarctic environment, Kilpisjarvi, Finland. Arct Alp Res 20:97–105

Corner GD (1980) Avalanche impact landforms in Troms, North Norway. Geogr Ann Ser (Phys Geogr) 62:1–4

Corner GD (2005a) Scandes mountains. In: Seppälä M (ed) The physical geography of Fennoscandia. Wiley-Blackwell, Chichester, pp 229–254

Corner GD (2005b) Atlantic coasts and fjords. In: Seppälä M (ed) The physical geography of Fennoscandia. Wiley-Blackwell, Chichester, pp 203–228

Costa JE (1984) Physical geomorphology of debris flows. In: Costa JE, Fleisher PJ (eds) Developments and applications of geomorphology. Springer Verlag, Berlin, pp 268–317

Curry AM (1999) Paraglacial modification of slope form. Earth Surf Proc Land 24:1213–1228

Curry AM (2000) Observations on the distribution of paraglacial reworking of glacigenic drift in western Norway. Nor Geogr Tidsskr 54:139–147

Curry AM (2021) Paraglacial rock-slope failure following deglaciation in Western Norway. In Beylich AA (ed) Landscapes and landforms of Norway. Springer Nature: Cham, pp 97–130.

Curry AM, Ballantyne CK (1999) Paraglacial modification of glacigenic sediments. Geogr Ann Ser (Phys Geogr) 81:409–419

Darmody RG, Thorn CE (1997) Elevation, age, soil development, and chemical weathering at Storbreen, Jotunheimen. Geogr Ann Ser (Phys Geogr) 79:215–222

Darmody RG, Thorn CE, Harder RL, Schlyter JPL, Dixon JC (2000) Weathering implications of water chemistry in an arctic-alpine environment, northern Sweden. Geomorphology 34:89–100

Darmody RG, Thorn CE, Seppålå M, Campbell SW, Li YK, Harbor J (2008) Age and weathering status of granite tors in Arctic Finland (~68°N). Geomorphology 94:10–23

Dawson AG (1979) Polar and non-polar shore platform development. Department of Geography, Bedford College (University of London). Pap Geogr 6:1–28

Dawson AG, Matthews JA, Shakesby RA (1987) Rock platform erosion on periglacial shores: a modern analogue for Pleistocene rock platforms in Britain. In: Boardman J (ed) Periglacial processes and landforms in Britain and Ireland. Cambridge University Press, Cambridge, pp 173–182

De Haas T, Kleinhaus MG, Carbonneau PE, Rubensdottir L, Hauber E (2015) Morphology of fans in the high-arctic periglacial environment of Svalbard: controls and processes. Earth Sci Rev 146:163–182

Decaulne A, Eggertsson Ó, Laute K, Beylich AA (2014) A 100-year extreme snow-avalanche record based on tree-ring rsearch in upper Bødalen, inner Nordfjord, western Norway. Geomorphology 218:3–15

Demek J (1969) Cryoplanation terraces, their geographical distribution, genesis and development. Rozpravy Ĉeskoslovenské Akademie Věd, Rada Matematických a Prírodních Věd Rocnik 79(4):1–80

Eichel J, Draebling D, Klingbeil L, Wieland M, Wling C, Schmidtlein S, Kuhlmann H, Dikau R (2017) Solifluction meets vegetation: the role of biogeomorphic feedbacks for turf-banked solifluction lobe development. Earth Surf Proc Land 42:1623–1635

Elliott G, Worsley P (1999) The sedimentology, stratigraphy and ^{14}C dating of a turf-banked solifluction lobe: evidence for Holocene slope instability at Okstindan, northern Norway. J Quat Sci 14:175–188

Elliott G, Worsley P (2012) A solifluction lobe in Okstindan, north Norway and its paleoclimatic significance. In: Eberhardt E, Froese C, Turner K, Leroueil S (eds) Landslides and engineering slopes: protecting society through improved understanding. Taylor & Francis, London, pp 437–442

Ellis S (1979) Radiocarbon dating evidence for the initiation of solifluction ca. 5500 years B.P. at Okstindan, north Norway. Geogr Ann Ser (Phys Geogr) 61:29–33

Ellis S (1983) Stratigraphy and ^{14}C dating of two earth hummocks, Jotunheimen, south central Norway. Geogr Ann Ser (Phys Geogr) 65:279–287

Engeland K, Aano A, Steffensen I, Støren E, Paasche Ø (2020) New flood frequency estimates for the largest river in Norway based on the combination of short and long time series. Hydrol Earth Syst Sci 24:5595–5619

Enquist F (1916) Die Einfluss des Windes auf die Verteilung der Gletscher. Bull Geol Inst Univ Upps 14:1–108

Eriksen HØ, Rouyet L, Lauknes TR, Berthling I, Isaksen K, Hindberg H, Larsen Y, Corner GD (2018) Recent acceleration of a rock glacier complex, Ádjet, Norway, documented by 62 years of remote sensing observations. Geophys Res Lett 45(16):8314–8323

Etzelmüller B, Berthling I, Sollid JL (2003) Aspects and concepts on the geomorphological significance of Holocene permafrost in southern Norway. Geomorphology 52:87–104

Etzelmüller B, Hagen JO (2005) Glacier-permafrost interaction in Arctic and alpine mountain environments with examples from southern Norway and Svalbard. In Harris C, Murton JB (eds) Cryospheric systems: glaciers and permafrost, vol 242. Geological Society, London, Special Publication, pp 11–27

Etzelmüller B, Romstad B, Fjellanger J (2007) Automated regional classification of topography in Norway. Norw J Geol 87:167–180

Etzelmüller B, Guglielmin M, Hauck C, Hilbich C, Hoelzle M, Isaksen K, Noetzli J, Oliva M, Ramos M (2020) Twenty years of European mountain permafrost dynamics–the PACE legacy. Environ Res Lett 15: Article No. 104070.

Etzelmüller B, Czekirda J, Magnin F, Duvillard P-A, Malet E, Ravanel L, Aspaas A, Kristensen L, Skrede I, Majala D, Jacobs B, Leinauer J, Hauck C, Hilbich C, Böhme M, Hermanns R, Eriksen HØ, Krautblatter M, Westermann S (2021) Permafrost in monitored unstable rock slopes in Norway—new insights from rock wall temperature monitoring, geophysical surveying and numerical modelling. Earth Surf Dyn Discuss. https://doi.org/10.5194/esurf-2021-10

Fabel B, Stroeven AP, Harbor J, Kleman J, Elmore D, Fink D (2002) Landscape preservation under Fennoscandian ice sheets determined from *in situ* produced ^{10}Be and ^{26}Al. Earth Planet Sci Lett 201:397–406

Farbrot H, Hipp TF, Etzelmüller B, Isaksen K, Ødegård RS, Schuler TV, Humlum O (2011) Air and ground-temperature variations observed along elevation and continentality gradients in southern Norway. Permafrost Periglac Process 22:343–360

Fredin O (2002) Glacial incepton and Quaternary mountain glaciations in Fennoscandia. Quat Int 95–96:99–112

Fredin O, Viola G, Zwingmann H, Sørlie R, Brönner M, Lie J-E, Grandal EM, Müller A, Margreth A, Vogt C, Knies J (2017) The inheritance of a Mesozoic landscape in western Scandinavia. Nature Communications 8: Article No. 14879, pp 1–11.

French HM (2008) Periglacial processes and forms. In: Burt TP, Chorley RJ, Brunsden D, Cox NJ, Goudie AS (eds) The history of the study of landforms or the development of geomorphology, vol 4. The Geological Society, London, pp 622–676

French HM (2018) The periglacial environment. Wiley-Blackwell, Chichester

French HM, Karte J (1988) A periglacial overview. In: Clark MJ (ed) Advances in periglacial geomorphology. Wiley, Chichester, pp 463–473
French HM, Thorn CE (2006) The changing nature of periglacial geomorphology. Géomorphologie: Relief Process Environ 3:165–174
Fries TCE, Bergström E (1910) Några iakttagelser öfver palsar och deras förekomst i nordligaste Sverige. Geol Föreningen I Stock Förhandlingar 32:195–205
Fronzek S, Luoto M, Carter TR (2006) Potential effect of climate change on the distribution of palsa mires in subarctic Fennoscandia. Climate Res 32:1–12
Fronzek S, Carter TR, Räisänen J, Ruokolainen L, Luoto M (2010) Applying probabilistic projections of climate change with impact models: a case study for sub-arctic palsa mires in Fennoscandia. Clim Change 99:515–534
Gisnås K, Etzelmüller B, Lussana C, Hjort J, Sannel ABK, Isaksen K, Westermann S, Kuhry P. Christiansen H, Frampton A, Åkerman J (2017) Permafrost map for Norway, Sweden and Finland. Permafr Periglacial Process 28:359–378
Gjessing J (1967) Norway's palaeic surface. Nor Geogr Tidsskr 21:69–132
Goodfellow BW (2012) A granulometry and secondary mineral fingerprint of chemical weathering in periglacial landscapes and its application to blockfield origins. Quat Sci Rev 57:121–135
Goodfellow BW, Strøeven AP, Fabel D, Fredin O, Derron M-H, Bintanja R, Caffee MW (2014) Arctic-alpine blockfields in the northern Swedish Scandes: late Quaternary—not Neogene. Earth Surf Dyn 2:383–401
Grab S (2005) Aspects of the geomorphology, genesis and environmental significance of earth hummocks (thúfur, pounus): miniature cryogenic mounds. Prog Phys Geogr 29:139–155
Guilcher A, Bodéré J-C, Coudé A, Hansom JD, Moign A, Peulvast J-P (1986) Le problème des strandflats en cinq pays de hautes latitudes. Rev Géol Dynam Géog Phys 27:47–79
Gurney SD (2001) Aspects of the genesis, geomorphology and terminology of palsas: perennial cryogenic mounds. Prog Phys Geogr 25:249–260
Haeberli W (1985) Creep of mountain permafrost: internal structure and flow of alpine rock glaciers. Mitteilungen der Versuchsanstalt für Wasserbau, Hydrologie und Glaziologie 77:1–142
Hall K (1998) Nivation or cryoplanation: different terms, same features? Polar Geogr 22:1–16
Hansom JD, Forbes DL, Etienne S (2014) The rock coasts of polar and sub-polar regions. In Kennedy DM, Stephenson JJ, Naylor LA (eds) Rock coast geomorphology: a global synthesis, vol 40. Geological Society of London, Memoirs, pp 263–281
Harris C (1982) The distribution and altitudinal zonation of periglacial landforms, Okstindan, Norway. Zeitschrift Für Geomorphologie NF 26:283–304
Harris C (1986) Some observations concerning the morphology and sedimentology of a protalus rampart, Okstindan, Norway. Earth Surf Proc Land 11:673–676
Harris C, Matthews JA (1984) Some observations on boulder-cored frost boils. Geogr J 150:63–73
Harris C, Murton JB (2005) Interactions between glaciers and permafrost: an introduction. In Harris C, Murton JB (eds) Cryospheric systems: glaciers and permafrost, vol 242. Geological Society, London, Special Publication, pp 1–9
Harris C, Kern-Luetschg M, Smith F, Isaksen K (2008) Solifluction processes in an area of seasonal ground freezing, Dovrefjell, Norway. Permafrost Periglac Process 19:31–47
Harris C, Arenson LU, Christiansen HH, Etzelmüller B, Frauenfelder R, Gruber S, Haeberli W, Hauck C, Hoelzle M, Humlum O, Isaksen K, Kääb A, Kern-Luetschg MA, Lehning M, Matsuoka N, Murton JB, Noezli J, Phillips M, Ross N, Seppälä M, Springman SM, Vonder Mühll DV (2009) Permafrost and climate in Europe: monitoring and modelling thermal, geomorphological and geotechnical responses. Earth-Sci Rev 92:117–171
Harris SA, Brouchkov A, Guodong C (2018) Geocryology: characteristics and use of frozen ground and permafrost landforms. CRC Press-Balkema, Leiden
Hättestrand C, Stroeven AP (2002) A relict landscape in the centre of the Fennoscandian glaciation: geomorphological evidence of minimal Quaternary glacial erosion. Geomorphology 44:127–143
Haugland JE (2004) Formation of patterned ground and fine-scale soil development within two late Holocene glacial chronosequences: Jotunheimen, Norway. Geomorphology 61:287–301

Haugland JE (2006) Short-term periglacial processes, vegetation succession, and soil development within sorted patterned ground: Jotunheimen, Norway. Arct, Antarct AlpE Res 38:82–89
Haugland JE, Beaty SW (2005) Vegetation establishment, succession and microsite frost disturbance on glacier forelands within patterned ground chronosequences. J Biogeogr 32:145–153
Haugland JE, Owen BS (2005) Temporal and spatial variability of soil pH in patterned ground chronosequences: Jotunheimen, Norway. Phys Geogr 26:299–312
Haugland JE, Owen-Haugland BS (2008) Cryogenic disturbance and pedogenic lag effects as determined by profile developmental index: the Styggedalsbreen glacier chronosequence, Norway. Geomorphology 96:212–220
Heckmann T, Morche D (eds) (2019) Geomorphology of proglacial systems: landforms and sediment dynamics in recently deglaciated alpine landscapes. Springer Nature, Cham.
Heikkinen O (2005) Boreal forest and northern and upper timberlines. In: Seppålå M (ed) The physical geography of Fennoscandia. Wiley-Blackwell, Chichester, pp 185–200
Heisser M, Scheidl C, Eisl J, Spangl B, Hübl J (2015) Process type identification in torrential catchments in the eastern Swiss Alps. Geomorphology 232:239–247
Henderson IHC, Saintot (2011) Regional spatial variations in rockslide distribution from structural geology ranking: an example from Storfjorden, western Norway. In Jaboyedoff M (ed) Slope tectonics, vol 351. Geology Society of London, Special Publications, pp 59–70
Hermanns RL, Schleier M, Böhme M, Blikra LH, Gosse K, Ivy-Ochs S, Hilger P (2017) Rock-avalanche activity in W and S Norway peaks after the retreat of the Scandinavian ice sheet. In: Mikos M, Vilímek V, Yin Y, Sassa K (eds) Advancing culture of living with landslides, volume 5: Landslides in different environments. Springer, Heidelberg, pp 331–338
Hilger P, Hermanns RL, Gosse JC, Jacobs B, Etzelmüller B, Krautblatter M (2018) Multiple rock-slope failures from Mannen in Romsdal Valley, western Norway, revealed from Quaternary geological mapping and ^{10}Be exposure dating. Holocene 28:1841–1854
Hilger P, Hermanns RL, Czekirda J, Myhra KS, Gosse JC, Etzelmüller B (2021) Permafrost as a first order control on long-term rock-slope deformation in (Sub-) Arctic Norway. Quat Sci Rev 251:1–21. Article No. 106718
Hipp T, Etzelmüller B, Westermann S (2014) Permafrost in alpine rock faces from Jotunheimen and Hurrungane, southern Norway. Permafrost Periglac Process 25:1–13
Hjort J (2006) Environmental factors affecting the occurrence of periglacial landforms in Finnish Lapland: a numerical approach. Shaker Verlag, Aachen
Hjort J (2014) Which environmental factors determine recent cryoturbation and solifluction activity in a subarctic landscape? A comparison between active and inactive features. Permafrost Periglac Process 25:136–143
Högbom B (1914) Über die geologische Bedeutung des Frostes. Bull Geol Inst Univ Upps 12:251–389
Högbom I (1923) Ancient inland dunes of northern and middle Europe. Geogr Ann 5:113–242
Högbom B (1927) Beobachtungen aus Nord-Schweden über den Frost als geologischer Factor. Bull Geol Inst Univ Upps 20:1–38
Hole PA (1981) Groper danna av snøskred I Sunnylven og tilgrensande områder på Sunnmøre. Førbels resultat. Norsk Geografiske Tidsskrift 35:167–172
Holtedahl O (1960) Features of the geomorphology. In Holtedahl O (ed) Geology of Norway. Norges Geologiske Undersøkelse, Trondheim, pp 507–531
Holtedahl O (1998) The Norwegian strandflat—a geomorphological puzzle. Nor Geol Tidsskr 78:47–66
Hughes AL, Gyllencreutz R, Lohne ØS, Mangerud J, Svendsen JI (2016) The last Eurasian ice sheets—a chronological database and time-slice reconstruction, DATED-1. Boreas 45:1–45
Humlum O (2008) Alpine and polar periglacial processes: the current state of knowledge. In Kane DL, Hinkel KM (eds) Ninth International Conference on Permafrost, Fairbanks, Alaska, June 29–July 3 2008, pp 753–759
Isaksen K, Holmlund P, Sollid JL, Harris C (2001) Three deep alpine permafrost boreholes in Svalbard and Scandinavia. Permafrost Periglac Process 12:13–26

Isaksen K, Hauck C, Gudevang E, Ødegård RS, Sollid JL (2002) Mountain permafrost distribution in Dovrefjell and Jotunheimen, southern Norway, based on BTS and DC resistivity tomography data. Nor Geogr Tidsskr 56:122–136

Jonasson C (1991) Holocene slope processes of periglacial mountain areas in Scandinavia and Poland. Uppsala Universitet Naturgeografiska Institutionen Report 79:1–156

Jonasson C, Nyberg R, Rapp A (1997) Dating of rapid mass movements in Scandinavia: talus rockfalls, debris flows and slush avalanches. In Matthews JA, Brunsden D, Frenzel B, Gläser B, Weiß (eds) Rapid mass movement as a source of climatic evidence for the Holocene. Gustav Fischer Verlag: Stuttgart, pp 267–282

Juliussen H, Humlum O (2007) Preservation of blockfields beneath Pleistocene ice sheets on Sølen and Elgåhogna, central eastern Norway. Z Geomorphol Suppl 51:113–138

Kääb A (2013) Rock glaciers and protalus forms. In: Elias SA (ed) Encyclopedia of Quaternary Science, vol 3, 2nd edn. Elsevier, Amterdam, pp 535–541

Karjalainen O, Aalto J, Luoto M, Westermann S, Romanovsky VE, Nelson FE, Etzelmüller B, Hjort J (2019) Circunpolar permafrost maps and geohazard indices for near-future infrastructure risk assessment. Sci Data 6(1):1–6

Karjalainen O, Luoto M, Aalto J, Etzelmüller B, Grosse G, Jones BM, Lilleøren KS, Hjort J (2020) High potential for loss of permafrost landforms in a changing climate. Environ Res Lett 15(10):104065

Karlén W (1988) Scandinavian glacier and climatic fluctuations during the Holocene. Quat Sci Rev 7:199–208

Käyhkö JA, Worsley P, Pye K, Clarke ML (1999) A revised chronology for aeolian activity in subarctic Fennoscandia during the Holocene. Holocene 9:195–205

Kejonen A (1979) Vuotomaista Muotkatunterien alueella Pohjois-Lapissa. Publ Dep Quat Geol Univ Turku 40:1–43

Kergillec R (2015) Characteristics and altitudinal distribution of periglacial decay phenomena in the massif of Rondane, central Norway. Geogr Ann Ser (Phys Geogr) 97:299–315

King L (1984) Permafrost in Skandinavien Untersuchungsergebnisse aus Lappland, Jotunheimen und Dovre/Rondane. Heidelberger Geographische Arbeiten 76:1–174

King L (1986) Zonation and ecology of high mountain permafrost in Scandinavia. Geogr Ann Ser (Phys Geogr) 68:131–139

Kleman J (1992) The palimpsest glacial landscape in northwestern Sweden—late Weichselian deglaciation landforms and traces of older west-centred ice sheets. Geogr Ann Ser (Phys Geogr) 74:305–325

Kleman J (1994) Preservation of landforms under ice sheets and ice caps. Geomorphology 9:19–32

Kleman J, Hättestrand C (1999) Frozen-bed Fennoscandian and Laurentian ice sheets during the Last Glacial Maximum. Nature 402:63–66

Kleman J, Stroeven AP, Lundqvist J (2008) Patterns of Quaternary ice sheet erosion and deposition in Fennoscandia and a theoretical framework for explanation. Geomorphology 97:73–90

Klemsdal T (1969) Eolian forms in parts of Norway. Nor Geogr Tidsskr 23:49–66

Klemsdal T (1982) Coastal classification and the coast of Norway. Nor Geogr Tidsskr 36:129–152

Kolstrup E (2004) Stratigraphic and environmental implications of a large ice-wedge cast at Tjæreborg, Denmark. Permafrost Periglac Process 15:31–40

Kotilainen M (2004) Dune stratigraphy as an indicator of Holocene climatic change and human impact in northern Lapland, Finland. Ann Acad Sci Fenn: Geol-Geogr 166:1–156

Kristensen L, Czekirda J, Penna I, Etzelmüller B, Nicolet P, Pullarello JS, Blikra LH, Skrede I, Oldani S, Abellan A (2021) Movements, failure and climatic control of the Veslemannen rockslide, Western Norway. Landslides. https://doi.org/10.1007/s10346-020-01609-x

Lauriol B, Lamirande I, Lalonde AE (2006) The Giant Steps of Bug Creek, Richardson Mountains, N.W.T., Canada. Permafr Periglac Process 17:267–275

Lautridou JP, Ozouf JC (1982) Experimental frost shattering: 15 years of research in the Centre de Géomorphologie du CNRS. Prog Phys Geogr 6:215–232

Larsen E, Holtedahl H (1985) The Norwegian strandflat: a reconsideration of its age and origin. Nor Geol Tidsskr 65:247–254

Lewis SG, Birnie JF (2001) Little Ice Age alluvial fan development in Langedalen, western Norway. Geogr Ann Ser (Phys Geogr) 83:179–190

Lidmar-Bergström K, Ollier CD, Sulebak JR (2000) Landforms and uplift history of southern Norway. Global Planet Change 24:211–231

Liestøl O (1974) Avalanche plunge-pool effect. Norsk Polarinstitutt Arbok 1972:179–181

Lilleøren KS, Etzelmüller B (2011) A regional inventory of rock glaciers and ice-cored moraines in Norway. Geogr Ann Ser (Phys Geogr) 93:175–191

Lilleoren KS, Etzelmuller B, Rouyet L, Eiken T, Hilbich C (2022) Transitional rock glaciers at sea-level in Northern Norway. Earth Surface Dynanics 6

Lilleøren KS, Etzelmüller B, Schuler TV, Gisnås K, Humlum O (2012) The relative age of mountain permafrost—estimation of Holocene permafrost limits in Norway. Global Planet Change 92–93:209–223

Lind L, Nilsson C, Polvi LE, Weber C (2014) The role of ice dynamics in shaping vegetation in flowing waters. Biol Rev 89:791–804

Linge H, Nesje A, Matthews JA, Fabel D, Xu S (2020) Evidence for rapid paraglacial formation of rock glaciers in southern Norway from ^{10}Be surface-exposure dating. Quat Res 97:55–70

Liston GE, Elder K (2006) A distributed snow-evolution modelling system. J Hydrometeorol 7:1259–1276

Longva O, Blikra LH, Dehls JF (2009) Rock avalanches—distribution and frequencies in the inner part of Storfjorden, Møre og Romsdal County, Norway. NGU Rapport 2009.002. Geological Survey of Norway: Trondheim

Lundqvist J (1964) Patterned ground and related forest phenomena in Sweden. Sveriges Geologiska Unersökning Avhandlingar och Uppsatser Ser. C 583, pp 1–101

Luoto M, Seppälä M (2002a) Characteristics of earth hummocks (pounus) with and without permafrost in Finnish Lapland. Geogr Ann Ser (Phys Geogr) 84:127–136

Luoto M, Seppälä M (2002b) Modelling the distribution of palsas in Finnish Lapland with logistic regression and GIS. Permafrost Periglac Process 13:17–28

Luoto M, Seppålå M (2003) Thermokarst ponds as indicators of the former distribution of palsas in Finnish Lapland. Permafrost Periglac Process 14:19–27

Magnin F, Etzelmüller B, Westermann S, Isaksen K, Hilger P, Hermanns RL (2019) Permafrost distribution in steep rock slopes in Norway: measurements, statistical modelling and implications for geomorphic processes. Earth Surf Dyn 7:1019–1040

Mangerud J, Aarseth I, Hughes ALC, Lohne ØS, Skår K, Sønstegaard E, Svendsen JI (2016) A major re-growth of the Scandinavian Ice Sheet in western Norway during the Allerød-Younger Dryas. Quat Sci Rev 132:175–205

Margold M, Treml V, Petr L, Nyplová P (2011) Snowpatch hollows and pronival ramparts in the Krkonose Mountains, Czech Republic: distribution, morphology and chronology of formation. Geogr Ann Ser (Phys Geogr) 93:137–150

Marr P, Löffler G (2018) Establishing a multi-proxy approach to alpine blockfield evolution in south-central Norway. Acta Univ Carol Geogr 52:219–236

Marr P, Winkler S, Löffler G (2018) Investigations on blockfields and related landforms at Blåhø (southern Norway) using Schmidt-hammer exposure-age dating: palaeoclimatic and morphodynamic implications. Geogr Ann Ser (Phys Geogr) 100:285–306

Marr P, Winkler S, Löffler G (2019) Schmidt-hammer exposure-age dating (SHD) performed on periglacial and related landforms in Oppendskedalen, Geirangerfjellet, Norway: implications for mid- and late-Holocene climate variability. Holocene 29:97–109

Matsuoka N (2001) Microgelivation versus macrogelivation: towards bridging the gap between laboratory and field frost weathering. Permafrost Periglac Process 12:299–313

Matthews JA (1985) Radiocarbon dating of surface and buried soils: principles, problems and prospects. In Richards KS, Arnett RR, Ellis S (eds) Geomorphology and soils. George Allen & Unwin, London, pp 269–288

Matthews JA (1992) The ecology of recently-deglaciated terrain: a geoecological approach to glacier forelands and primary succession. Cambridge University Press, Cambridge

Matthews JA (1993) Radiocarbon dating of buried soils with particular reference to Holocene solifluction. In: Frenzel B, Matthews JA, Gläser B (eds) Solifluction and climatic variation in the Holocene. Gustav Fischer Verlag, Stuttgart, pp 309–324

Matthews JA (1999) Disturbance regimes and ecosystem response on recently-deglaciated substrates. In: Walker R (ed) Ecosystems of disturbed ground. Elsevier, Amsterdam, pp 17–37

Matthews JA, Karlén W (1992) Asynchronous neoglaciation and Holocene climatic change reconstructed from Norwegian glaciolacustrine sedimentary sequences. Geology 20:991–994

Matthews JA, McCarroll D (1994) Snow-avalanche impact landforms in Breheimen, southern Norway: origin, age and paleoclimatic implications. Arct Alp Res 26:103–115

Matthews JA, Owen G (2008) Endolithic lichens, rapid biological weathering and Schmidt hammer R-values on recently exposed rock surfaces: Storbreen glacier foreland, Jotunheimen, Norway. Geogr Ann Ser (Phys Geogr) 90:187–297

Matthews JA, Owen G (2011) Holocene chemical weathering, surface lowering and rock weakening rates from glacially-eroded bedrock surfaces in an alpine periglacial environment, Jotunheimen, southern Norway. Permafrost Periglac Process 22:279–290

Matthews JA, Owen G (2021) The snow-avalanche impact landforms of Vestlandet, southern Norway. In: Beylich AA (ed) Landscapes and landforms of Norway. Springer, Berlin, pp 131–145

Matthews JA, Seppälä, M (2014) Holocene environmental change in subarctic aeolian dunefields: the chronology of sand dune re-activation events in relation to forest fires, palaeosol development and climatic variations in Finnish Lapland. Holocene 24:149–164

Matthews JA, Seppälä M (2015) Holocene colluvial chronology in a sub-arctic esker landscape at Kuttanen, Finnish Lapland: kettle holes as geo-ecological archives of interactions amongst fire, vegetation, soil, climate and geomorphological instability. Boreas 44:343–367

Matthews JA, Vater AE (2015) Pioneer zone geo-ecological change: observations from a chronosequence on the Storbreen glacier foreland, Jotunheimen, southern Norway. Catena 135:219–230

Matthews JA, Wilson P (2015) Improved Schmidt-hammer exposure ages for active and relict pronival ramparts in southern Norway and their palaeoenvironmental implications. Geomorphology 246:7–21

Matthews JA, Harris C, Ballantyne CK (1986a) Studies on a gelifluction lobe, Jotunheimen, Norway: ^{14}C chronology, stratigraphy, sedimentology and palaeoenvironment. Geogr Ann Ser (Phys Geogr) 86:345–360

Matthews JA, Dawson AG, Shakesby, RA (1986b) Lake shoreline development, frost weathering and rock platform erosion in an alpine periglacial environment. Boreas 15: 33-50.

Matthews JA, Dahl SO, Berrisford MS, Dresser PQ, Dumayne-Peaty L (1997a) A preliminary history of Holocene colluvial (debris-flow) activity, Leirdalen, Jotunheimen, Norway. J Quat Sci 12:117–129

Matthews JA, Dahl SO, Berrisford MS, Nesje A (1997b) Cyclic development and thermokarstic degradation of palsas in the mid-alpine zone at Leirpullan, Dovrefjell, southern Norway. Permafr Periglac Process 8:107–122

Matthews JA, Shakesby RA, Berrisford MS, McEwen LJ (1998) Periglacial patterned ground on the Styggedalsbreen glacier foreland, Jotunheimen, southern Norway: micro-topographic, paraglacial and geoecological controls. Permafrost Periglac Process 9:147–166

Matthews JA, Shakesby RA, McEwen LJ, Berrisford MS, Owen G, Bevan P (1999) Alpine debris flows in Leirdalen, Jotunheimen, Norway, with particular reference to distal fans, intermediate-type deposits and flow types. Arct Antarct Alp Res 31:421–435

Matthews JA, Seppälä M, Dresser PQ (2005) Holocene solifluction, climate variation and fire in a subarctic landscape at Pippokangas, Finnish Lapland, based on radiocarbon-dated buried charcoal. J Quat Sci 20:533–548

Matthews JA, Dahl SO, Dresser PQ, Berrisford MS, Lie Ø, Nesje A, Owen G (2009) Radiocarbon chronology of Holocene colluvial (debris-flow) events at Sletthamn, Jotunheimen, southern

Norway: a window on the changing frequency of extreme climatic events and their landscape impact. Holocene 19:1107–1129
Matthews JA, Shakesby RA, Owen G, Vater AE (2011) Pronival rampart formation in relation to snow-avalanche activity and Schmidt-hammer exposure-age dating (SHD): three case studies from southern Norway. Geomorphology 130:280–288
Matthews JA, Nesje A, Linge H (2013) Relict talus-foot rock glaciers at Øyberget, upper Ottadalen, southern Norway. Permafrost Periglac Process 24:336–346
Matthews JA, Winkler S, Wilson P (2014) Age and origin of ice-cored moraines in Jotunheimen and Breheimen, southern Norway: insights from Schmidt-hammer exposure-age dating. Geogr Ann Ser (Phys Geogr) 96:531–548
Matthews JA, McEwen LJ, Owen G (2015) Schmidt-hammer exposure-age dating (SHD) of snow-avalanche impact ramparts in southern Norway: approaches, results and implications for landform age, dynamics and developmemt. Earth Surf Landfs Process 40:1705–1718
Matthews JA, Wilson P, Mourne RW (2017a) Landform transitions from pronival ramparts to moraines and rock glaciers: a case study from Smørbotn cirque, Romsdalsalpane, southern Norway. Geogr Ann Ser (Phys Geogr) 99:15–37
Matthews JA, Owen G, McEwen LJ, Shakesby RA, Hill JL, Vater AE, Ratcliffe AC (2017b) Snow-avalanche impact craters in southern Norway: their morphology and dynamics compared with small terrestrial meteorite craters. Geomorphology 296:11–30
Matthews JA, Winkler S, Wilson P, Tomkins MD, Dortch JM, Mourne RW, Hill JL, Owen G, Vater A (2018) Small rock-slope failures conditioned by Holocene permafrost degradation: a new approach and conceptual model based on Schmidt-hammer exposure-age dating, Jotunheimen, southern Norway. Boreas 47:1144–1169
Matthews JA, Wilson P, Winkler S, Mourne RW, Hill JL, Owen G, Hiemstra J, Hallang H, Geary AP (2019) Age and development of active cryoplanation terraces in the alpine permafrost zone at Svartkampan, Jotunheimen, southern Norway. Quat Res 92:641–664
Matthews JA, Haselberger S, Hill JL, Owen G, Winkler S, Hiemstra JF, Hallang H (2020a) Snow-avalanche boulder fans in Jotunheimen, southern Norway: Schmidt-hammer exposure-age dating, geomorphometrics, dynamics and evolution. Geogr Ann Ser (Phys Geogr) 102:118–140
Matthews JA, McEwen LJ, Owen G, Los SO (2020b) Holocene alluvial fan evolution, Schmidt-hammer exposure-age dating and paraglacial debris floods in the SE Jostedalsbreen region, southern Norway. Boreas 49:886–904
Mauri A, Davis BAS, Collins PM, Kaplan JO (2015) The climate of Europe during the Holocene: a gridded pollen-based reconstruction and its multi-proxy evaluation. Quat Sci Rev 112:109–127
McCarroll D (1990) Differential weathering of feldspar and pyroxene in an arctic-alpine environment. Earth Surf Proc Land 15:641–651
McCarroll D, Viles HA (1995) Rock weathering by the lichen Lecidea auriculata in an arctic-alpine environment. Earth Surf Proc Land 20:199–206
McCarroll D, Shakesby RA, Matthews JA (1998) Spatial and temporal patterns of late-Holocene rockfall activity on a Norwegian talus slope: a lichenometric and simulation modelling approach. Arct Alp Res 30:51–60
McCarroll D, Shakesby RA, Matthews JA (2001) Enhanced rockfall activity during the Little Ice Age: further lichenometric evidence from Norwegian talus. Permafrost Periglac Process 12:157–164
McEwen LJ, Matthews JA (1998) Channel form, bed material and sediment sources of the Sprongdøla, southern Norway: evidence for a distinct periglacio-fluvial system. Geogr Ann Ser (Phys Geogr) 80:17–36
McEwen LJ, Matthews JA, Shakesby RA, Berrisford MS (2002) Holocene gorge excavation linked to boulder fan formation and frost weathering in a Norwegian alpine periglaciofluvial system. Arct Antarct Alp Res 34:345–357
McEwen LJ, Owen G, Matthews JA, Hiemstra JF (2011) Late-Holocene development of a Norwegian alluvial fan affected by proximal glacier variations, distal undercutting and colluvial activity. Geomorphology 127:198–215

McEwen LJ, Matthews JA, Owen G (2020) Development of a Holocene glacier-fed composite alluvial fan based on surface exposure-age dating techniques: the Illåe fan, Jotunheimen, Norway. Geomorphology 363: Article No. 107200 (15 p).
Mercier D (2008) Paraglacial and paraperiglacial land systems: concepts, temporal scales and spatial distribution. Geomorphol: Relief Process Environ 14:223–233
Miesen F, Dahl SO, Schrott L (2021) Evidence of glacier-permafrost interactions associated with hydro-geomorphologicasl processes and landforms at Snøhetta, Dovrefjell, Norway. Geogr Ann Ser (Phys Geogr) 103:273–302
Milthers V (1907) Sandslebne stens form og danelse. Meddelelser fra Dansk Geologiske Forening 13:3–60.
Moen A (1999) National Atlas of Norway: Vegetation. Norwegian Mapping Authority, Hønefoss.
Möller JJ, Sollid JL (1972) Deglaciation chronology of Lofoten-Vesterålen-Ofoten, North Norway. Norske Geografisk Tidsskrift 26:101–133
Murton JB (2021) What and where are periglacial landscapes. Permafr Periglac Process 32:186–212
Murton JB, Coutard J-P, Lautridou J-P, Ozouf J-C, Robinson DA, Williams RBG (2001) Physical modelling of bedrock brecciation by ice segregation in permafrost. Permafrost Periglac Process 12:255–266
Murton JB, Peterson R, Ozouf J-C (2005) Bedrock fracture by ice segregation in cold regions. Science 314:1127–1129
Nansen F (1922) The strandflat and isostasy. Videnskapselskapet I Christiania Skrifter, Matematisk-Naturvitenskapelig klasse 2:1–313
Nesje A (1993) Neoglacial gelifluction in the Jostedalsbre region, western Norway: evidence from dated buried soils. In: Frenzel B, Matthews JA, Gläser B (eds) Solifluction and climatic variation in the Holocene. Gustav Fischer Verlag, Stuttgart, pp 37–47
Nesje A, Kvamme M (1991) Holocene glacier and climatic variations in western Norway: evidence for early-Holocene demise and multiple Neoglacial events. Geology 19:610–612
Nesje A, Willans IM (1994) Erosion of Sognefjord, Norway. Geomorphology 9:33–45
Nesje A, Dahl SO, Anda E, Rye N (1988) Blockfields in southern Norway. Significance for the Late Weichselian ice sheets. Nor Geol Tidsskr 68:149–169
Nesje A, Kvamme M, Rye N (1989) Neoglacial gelifluction in the Jostedalsbreen region, western Norway: evidence from dated buried palaeopodsols. Earth Surf Proc Land 14:259–270
Nesje A, Kvamme M, Rye N, Løvlie R (1991) Holocene glacial and climatic history of the Jostedalsbreen region, western Norway: evidence from lake sediments and terrestrial deposits. Quat Sci Rev 10:87–114
Nesje A, Bakke J, Dahl SO, Lie Ø, Bøe AG (2007) A continuous, high-resolution 8500-yr snow-avalanche record from western Norway. Holocene 17:269–277
Nesje A, Matthews JA, Linge H, Bredal M, Wilson P, Winkler S (2021) New evidence for active talus-foot rock glaciers at Øyberget, southern Norway, and their development during the Holocene. Holocene 31 (in press)
Nicholson DT (2008) Rock control on microweathering of bedrock surfaces in a periglacial environment. Geomorphology 101:655–665
Nicholson DT (2009) Holocene microweathering rates and processes on ice-eroded bedrock, Røldal area, Hardangervidda, southern Norway. In Knight J, Harrison S (eds) Periglacial and paraglacial processes and environments, vol 320. Geological Society, London, Special Publication, pp 29–49
Nielsen PR, Dahl SO, Jansen HL, Støren EWN (2016a) Holocene aeolian sedimentation and episodic mass-wasting events recorded in lacustrine sediments on Langøya in Vesterålen, northern Norway. Quat Sci Rev 148:146–162
Nielsen PR, Dahl SO, Jansen HL (2016b) Mid- to late-Holocene aeolian activity recorded in a coastal dunefield and lacustrine sediments on Andøya, northern Norway. Holocene 26:1486–1501
Niessen A, van Horssen P, Koster EA (1992) Altitudinal zonation of selected geomorphological phenomena in an alpine perglacial area (Abisko, northern Sweden). Geogr Ann Ser (Phys Geogr) 74:1835–2196

Nihlén T (2003) Palsas at Härjedalen, Sweden: 1910 and 1998 compared. Geogr Ann Ser (Phys Geogr) 82:39–44

Nyberg R (1985) Debris flows and slush avalanches in northern Swedish Lappland: distribution and geomorphological significance. Meddelanden Frå Lunds Universitets Geografiska Institution Avhandlingar 97:1–144

Nyberg R (1989) Observations of slushflows and their geomorphological effects in the Swedish mountain area. Geogr Ann Ser (Phys Geogr) 71:185–198

Nyberg R (1991) Geomorphic processes at snowpatch sites in the Abisko Mountains, northern Sweden. Zeitschrift für Geomorphologie N.F. 35: 321–343

Nyland K, Nelson FE, Figueiredo PM (2020) Cosmogenic ^{10}Be and ^{36}Cl geochronology of cryoplanation terraces in the Alaskan Yukon-Tanana upland. Quat Res 97:157–166

Ødegård RS, Sollid JL, Liestøl O (1987) Juvflya – Kvartærgeologi og geomorfologi M 1:10.000. Geografisk Institutt, Universitetet I Oslo, Oslo

Ødegård RS, Sollid JL, Liestøl O (1988) Periglacial forms related to terrain parameters in Jotunheimen, southern Norway. In: Senneset K (ed) 5th International Conference on Permafrost, Proceedings, vol 3. Tapir, Trondheim, pp 59–61

Ødegård RS, Sollid JL, Liestøl O (1992) Ground temperature measurements in mountain permafrost, Jotunheimen, southern Norway. Permafrost Periglac Process 3:231–234

Ødegård RS, Sollid JL (1993) Coastal cliff temperatures related to the potential for cryogenic weathering processes, western Spitsbergen, Svalbard. Polar Res 12:95–106

Ojala AEK, Mattila J, Markovaara-Koivisto M, Ruskeeniemi T, Palmu J-P, Sutinen R (2019) Distribution and morphology of landslides in northern Finland: an analysis of postglacial seismic activity. Geomorphology 326:190–121

Oksanen PO (2005) Development of palsa mires on the northern European continent in relation to Holocene climatic and environmental changes (Academic dissertation). Oulu University Press, Oulu, pp 1–50

Oksanen PO (2006) Holocene development of the Vaisjeäggi palsa mire, Finnish Lapland. Boreas 35:81–95

Olesen O, Bering D, Brönner M, Dalsegg E, Fabian K, Fredin O, Gellein J, Husteli B, Magnus C, Rønning JS, Solbakk T, Tønnesen JF, Øverland JA (2012) Tropical weathering in Norway. Norwegian Geological Survey Report 2012.005, 188 p

Olesen O, Kierulf HP, Brönner M, Dalsegg E, Fredin O, Solbakk T (2013) Deep weathering, neotectonics and strandflat formation in Nordland, northern Norway. Norw J Geol 93:189–213

Olvmo M, Holmer B, Thorsson S, Reese H, Lindberg F (2020) Sub-arctic palsa degradation and the role of climatic drivers in the largest coherent palsa mire complex in Sweden (Vissátvuopmi), 1955–2016. Scientific Reports Article No. 10: 8937 (10 p). https://doi.org/10.1038/s41598-020-65719-1

Oppikofer T, Saintot A, Hermanns RL, Böhme M, Scheiber T, Gosse J, Dreiås GM (2017) From incipient slope instability through slope deformation to catastrophic failure—different stages of failure development on the Ivasnasen and Vollan rock slopes (western Norway). Geomorphology 289:96–116

Østrem G (1959) Ice melting under a thin layer of moraine, and the existence of ice cores in moraine ridges. Geogr Ann 41:228–230

Østrem G (1964) Ice-cored moraines in Scandinavia. Geogr Ann 46:282–337

Østrem G (1965) Problems of dating ice-cored moraines. Geogr Ann 47:1–38

Østrem G (1971) Rock glaciers and ice-cored moraines: a reply to D. Barsch. Geogr Ann Ser (Phys Geogr) 53:207–213

Ouellet M-A, Germain D (2014) Hyperconcentrated flows on a forested alluvial fan of eastern Canada: geomorphic characteristics, return period and triggering scenarios. Earth Surf Proc Land 39:1876–1887

Owen G, Matthews JA, Shakesby RA, He X (2006a) Snow-avalanche impact landforms, deposits and effects at Urdvatnet, southern Norway: implications for avalanche style and process. Geogr Ann Ser (Phys Geogr) 88:295–307

Owen G, Matthews JA, Shakesby RA (2006b) Holocene chemical weathering on a calcitic lake shoreline in an alpine periglacial environment: Attgløyma, Sognefjell, southern Norway. Permafr Periglac Process 17:3–12
Owen G, Matthews JA, Albert PG (2007) Rates of Holocene chemical weathering, 'Little Ice Age' glacial erosion, and implications for Schmidt-hammer dating at a glacier-foreland boundary, Fåbergstølsbreen, southern Norway. Holocene 17:829–834
Paasche Ø, Strømsøe JR, Dahl SO, Linge H (2006) Weathering characteristics of arctic islands in northern Norway. Geomorphology 82:430–452
Paasche Ø, Dahl SO, Løvlie R, Bakke J, Nesje A (2007) Rockglacier activity during the Last Glacial-Interglacial transition and Holocene spring snowmelting. Quat Sci Rev 26:793–807
Pierson TC (2005) Hyperconcentrated flow—transitional process between water flow and debris flow. In: Jakob M, Hungr O (eds) Debris flows/avalanches. Geological Society of America, Boulder CO, pp 1–12
Pissart A (2002) Palsas, lithalsas and remnants of these periglacial mounds. A progress report. Prog Phys Geogr 26:605–621
Pissart A (2013) Palsas and lithalsas. In: Giardino JR, Harbor JM (eds) Treatise on geomorphology, volume 8, glacial and periglacial geomorphology. Academic Press, San Diego CA, pp 223–237
Porter SC (1989) Some geological implications of average Quaternary glacial conditions. Quat Res 32:245–261
Priesnitz K (1988) Cryoplanation. In: Clark MJ (ed) Advances in periglacial geomorphology. Wiley, Chichester, pp 49–67
Rapp A (1957) Studien über schutthalden in Lappland und auf Spitzbergen. Zeitschrift für Geomorphologie NF 1:179–200
Rapp A (1959) Avalanche boulder tongues in Lappland. Geogr Ann 41:34–48
Rapp A (1960) Recent development of mountain slopes in Kärkevagge and surroundings, northern Scandinavia. Geogr Ann 42:65–200
Rapp A (1982) Zonation of permafrost indicators in Swedish Lappland. Geogr Tidsskr/Dan J Geogr 82:37–38
Rapp A (1984) Nivation hollows and glacial cirques in Söderåsen, Scania, south Sweden. Geogr Ann Ser (Phys Geogr) 66:11–28
Rapp A, Åkerman HJ (1993) Slope processes and climate in the Abisko Mountains, northern Sweden. In: Frenzel B, Matthews JA, Gläser B (eds) Soliflucton and climatic variation in the Holocene. Gustav Fischer Verlag, Stuttgart, pp 163–177
Rapp A, Clark M (1971) Large nonsorted polygons in Padjelanta National Park, Swedish Lappland. Geogr Ann Ser (Phys Geogr) 53:71–85
Rapp A, Nyberg R (1988) Mass movements, nivation processes and climatic fluctuations in northern Scandinavian mountains. Nor Geogr Tidsskr/Nor J Geogr 42:245–253
Rasmussen A (1981) The deglaciation of the coastal area NW of Svartisen, Northern Norway. Nor Geol Unders 369:1–31
Rea BR, Whalley WB, Rainey MM, Gordon JE (1996) Blockfields old or new? Evidence and implications for some plateaus in northern Norway. Geomorphology 15:109–121
Reid JR, Nesje A (1988) A giant ploughing block, Finse, southern Norway. Geogr Ann Ser (Phys Geogr) 70:27–33
Reusch H (1894) Strandfladen, et nyt træk i Norges geografi. Norges Geologiske Undersøgelse 14:1–14
Ridefelt H, Boelhouwers J (2006) Observations on regional variation in solifluction landform morphology and environment in the Abisko region, northern Sweden. Permafrost Periglac Process 17:253–266
Ridefelt H, Åkerman J, Beylich A, Boelhouwers J, Kolstrup E, Nyberg R (2009) 56 years of solifluction measurements in the Abisko mountains, northern Sweden—analysis of temporal and spatial variations of slow soil surface movements. Geogr Ann Ser (Phys Geogr) 91: 215–232
Rikkinen J (1989) Relations between topography, microclimates and vegetation in the Kalmari-Saarijarvi esker chain, central Finland. Fennia 167:87–150

Rönkkö M, Seppälä M (2003) Surface characteristics affecting active layer formation in palsas, Finnish Lapland. In: Phillips M, Springman SM, Arenson LU (eds) Permafrost: Proceedings of the Eighth International Conference on Permafrost. Swets and Zeitlinger, Lisse, pp 995–1000
Rubensdotter l, Sletten K, Sandøy G (2021) Morphological description of erosional and depositional landfoms formed by debris flow processes in mainland Norway. In Beylich AA (ed) Landscapes and landforms of Norway. Berlin: Springer, pp 225–240
Rudberg S (1977) Periglacial zonation in Scandinavia. Abhandlungen der Akademie der Wissenschaften in Göttingen Mathematisch-Physikalische Klasse 31:92–104
Samuelsson C (1926) Studien über die Wirkungen des Windes in den kalten und gemässigten Erdteilen. Bull Geol Inst Univ Upps 20:57–230
Sannel ABK (2020) Ground temperature and snow depth variability within a subarctic peat plateau landscape. Permafrost Periglac Process 31:255–263
Sannel ABK, Kuhry P (2011) Warming-induced destabilization of peat plateau/thermokarst lake complexes. J Geophys Res 116:GO3035
Sannel ABK, Hugelius G, Jansson P, Kuhry P (2016) Permafrost warming in a subarctic peatland—which meteorological controls are most important? Permafr Periglac Process 27:177–188
Sandersen F (1997) The influence of meteorological factors on the initiation of debris flows in Norway. In Matthews JA, Brunsden D, Frenzel B, Gläser B, Weiß (eds) Rapid mass movement as a source of climatic evidence for the Holocene. Gustav Fischer Verlag: Stuttgart, pp 321–332
Sandvold S, Lie Ø, Nesje A, Dahl SO (2001) Holocene glacial and colluvial activity in Leirungsdalen, eastern Jotunheimen, south-central Norway. Norw J Geol 81:25–40
Scapozza C, Lambiel C, Baron L, Marescot L, Reynard E (2011) Internal structure and permafrost distribution in two alpine periglacial talus slopes, Valais, Swiss Alps. Geomorphology 132:208–221
Scarpozza C (2016) Evidence of paraglacial and paraperiglacial crisis in Alpine sediment transfer since the last glaciation (Tincino, Switzerland). Quaternaire 27:139–155
Schleier M, Hermanns RL, Gosse JC, Oppikofer T, Rohn J, Tønnesen AF (2017) Subaqueous rock-avalanche deposits exposed by post-glacial isostatic rebound, Innfjorddalen, Western Norway. Geomorphology 289:117–133
Schlyter P (1995) Ventifacts as palaeo-wind indicators in southern Scandinavia. Permafrost Periglac Process 6:207–219
Schunke E, Zoltai SC (1988) Earth hummocks (thufur). In: Clark MJ (ed) Advances in periglacial geomorphology. Wiley, Chichester, pp 231–245
Sellier D, Kerguillec R (2021) Characterization of scree slopes in the Rondane mountains (south-central Norway). In Beylich AA (ed) Landscapes and landforms of Norway. Springer Nature, Cham, pp 203–223
Seppälä M (1971) Evolution of eolian relief of the Kaamasjoki—Kiellajoki river basin in Finnish Lapland. Fennia 104:1–88
Seppälä M (1972) Location, morphology and orientation of inland dunes in northern Sweden. Geogr Ann Ser (Phys Geogr) 54:85–104
Seppälä M (1981) Forest fires as activator of geomorphic processes in Kuttanen esker-dune region, northernmost Finland. Fennia 159:221–228
Seppälä M (1982) Present day periglacial phenomena in northern Finland. Biul Peryglac 29:231–243
Seppälä M (1986) The origin of palsas. Geogr Ann Ser (Phys Geogr) 68:141–147
Seppälä M (1988) Palsas and related forms. In: Clark MJ (ed) Advances in periglacial geomorphology. Wiley, Chichester, pp 247–278
Seppälä M (1994) Snow depth controls palsa growth. Permafrost Periglac Process 5:283–299
Seppälä M (1995a) Deflation and redeposition of sand dunes in Finnish Lapland. Quat Sci Rev 14:799–809
Seppälä M (1995b) How to make a palsa: a field experiment on formation of permafrost. Z Geomorphol Suppl 99:91–96
Seppälä M (1997) Distribution of permafrost in Finland. Bull Geol Soc Finl 69:87–96

Seppälä M (2003) Surface abrasion of palsas by wind action in Finnish Lapland. Geomorphology 52:141–148

Seppälä M (2004) Wind as a geomorphic agent in cold climates. Cambridge University Press, Cambridge

Seppälä M (2005a) Periglacial environment. In: Seppälä M (ed) The physical geography of Fennoscandia. Wiley-Blackwell, Chichester, pp 349–364

Seppälä M (2005b) Dating of palsas. In Ojala AEK (ed) Quaternary studies in the northern and Arctic regions of Finland. Geological Survey of Finland Special Paper 40, pp 79–84

Seppälä M (2011) Synthesis of studies of palsa formation underlining the importance of local environmental and physical characteristics. Quat Res 75:366–370

Sernander R (1905) Flytjord I svenska fjälltrakter. En botanisk-geologisk undersökning. Geol Föreningen I Stock Förhandlingar 27:41–84

Shakesby RA (1997) Pronival (protalus) ramparts: a review of forms, processes, diagnostic criteria and palaeoenvironmental implications. Prog Phys Geogr 21:394–418

Shakesby RA, Matthews JA (1987) Frost weathering and rock platform erosion on periglacial shorelines: a test of a hypothesis. Nor Geol Tidsskr 67:203

Shakesby RA, Dawson AG, Matthews JA (1987) Rock glaciers, protalus ramparts and related phenomena, Rondane, Norway: a continuum of large-scale talus-derived landforms. Boreas 16:305–317

Shakesby RA, Matthews JA, McCarroll D (1995) Pronival ("protalus") ramparts in the Romsdalsalpane, southern Norway: forms, terms, subnival processes, and alternative mechanisms of formation. Arct Alp Res 27:271–282

Shakesby RA, Matthews JA, McEwen LJ, Berrisford MS (1999) Snow-push processes in pronival (protalus) rampart formation: geomorphological evidence from Smørbotn, Romsdalsalpane, southern Norway. Geogr Ann Ser (Phys Geogr) 81:31–45

Slaymaker O (1988) The distinctive attributes of debris torrents. Hydrol Sci J 33:567–573

Slaymaker O (1995) Introduction. In: Slaymaker O (ed) Steepland geomorphology. Wiley, Chichester, pp 1–6

Slaymaker O (2009) Proglacial, periglacial or paraglacial? In Knight J, Harrison S (eds) Periglacial and paraglacial processes and environments, vol 320. Geological Society, London, Special Publication, pp 71–84

Sletten K, Blikra LH (2007) Holocene colluvial (debris-flow and water-flow) processes in eastern Norway: stratigraphy, chronology and palaeoenvironmental implications. J Quat Sci 22:619–635

Sletten K, Blikra LH, Ballantyne CK, Nesje A, Dahl SO (2003) Holocene debris flows recognized in a lacustrine sedimentary succession: sedimentology, chronostratigraphy and cause of triggering. Holocene 13:907–920

Sollid JL, Sørbel L (1992) Rock glaciers in Svalbard and Norway. Permafrost Periglac Process 3:215–222

Sollid JL, Sørbel L (1994) Distribution of glacial landforms in southern Norway in relation to the thermal regime of the last continental ice sheet. Geogr Ann Ser (Phys Geogr) 76:25–35

Sollid JL, Sørbel L (1998) Palsa bogs as a climatic indicator—examples ffom Dovrefjell, southern Norway. Ambio 27:287–291

Sollid JL, Andersen S, Hamre N, Kjeldsen O, Salvigsen O, Sturød S, Tveitå T, Wilhelmsen A (1973) Deglaciation of Finnmark, North Norway. Nor Geogr Tidsskr 27:233–325

Sollid JL, Holmlund P, Isaksen K, Harris C (2000) Deep permafrost boreholes in western Svalbard, northern Sweden and southern Norway. Nor Geogr Tidsskr 54:186–191

Sørensen T (1935) Bodenformen und Pflanzendecke in Nordostgrönland. Meddelelser om Gronland 93(4):1–69

Steiger C, Etzelmüller B, Westermann S, Myyhra KS (2016) Modelling the permafrost distribution in steep rockwalls in Norway. Norw J Geol 96:329–341

Stevens T, Sechl D, Tziavaras C, Schneider R, Banak A, Andreucci S, Hattestrand M, Pascucci V (2022) Age, formation and significance of loess deosits in central Sweden. Earth Surf Process Landf. https://doi.org/10.1002/esp.5456

Støren EN, Dahl SO, Lie Ø (2008) Separation of late-Holocene episodic paraglacial events and glacier fluctuations in eastern Jotunheimen, central southern Norway. Holocene 18:1179–1191
Støren EN, Dahl SO, Nesje A, Paasche Ø (2010) Identifying the sedimentary imprint of high-frequency Holocene river floods in lake sediments: development and application of a new method. Quat Sci Rev 29:3021–3033
Støren EN, Kolstad EW, Paasche Ø (2014) Linking past flood frequencies in Norway to regional atmospheric circulation anomalies. J Quat Sci 27:71–80
Strand SM, Christiansen HH, Johansson M, Åkerman J, Humlum O (2020) Active layer thickening and controls on interannual variability in the Nordic Arctic compared to the circum-Arctic. Permafrost Periglac Process 32:47–58
Strøeven AP, Fabel D, Hättestrand C, Harbor J (2002) A relict landscape in the centre of Fennoscandian glaciation: cosmogenic radionuclide evidence of tors preserved through multiple glacial cycles. Geomorphology 44:145–154
Strøeven AP, Hättestrand C, Kleman J, Heyman J, Fabel D, Fredin O, Goodfellow BW, Harbor JM, Jansen JD, Olsen L, Caffee MW, Fink D, Lundqvist J, Rosqvist GC, Strömberg B, Jansson KN (2016) Deglaciation of Fennoscandia. Quat Sci Rev 147:91–121
Strømsøe JR, Paasche Ø (2011) Weathering patterns in high-latitude regolith. J Geophys Res 116:F03021. https://doi.org/10.1029/2010JF001954
Sutinen R, Hyvönen E, Kukkonen I (2014) LiDAR detection of paleolandslides in the vicinity of the Suasselkä postglacial fault, Finnish Lapland. Int J Appl Earth Obs Geoinf 27:91–99
Svenonius FV (1909) Om scärf-eller blockhafven på våra högfjäll. Geol Föreningen I Stock Förhandlingar 32:169–181
Svensson H (1964) Tundra polygons. Photographic interpretation and field studies in North-Norwegian polygon areas. Norges Geologisk Undersøkelse Bulletin 223:298–327
Svensson H (1969) Open fissures in a polygonal net on the Norwegian Arctic coast. Biul Peryglac 19:389–398
Svensson H (1974) Distribution and chronology of relict polygon patterns on the Laholm Plain, the Swedish west coast. Geogr Ann Ser (Phys Geogr) 54:159–175
Svensson H (1983) Ventifacts as palaeowind indicators in a former periglacial area of southern Scandinavia. Proceedings of the Fourth International Conference on Permafrost, Fairbanks, Alaska, 18–22 July 1983, pp 1217–1220
Svensson H (1988) Ice-wedge casts and relict polygonal patterns in Scandinavia. J Quat Sci 3:57–68
Sverdrup HU (1938) Notes on erosion by drifting snow and transport of solid material by sea ice. Am J Sci 235:370–373
Thorn CE (1988) Nivation: a geomorphic chimera. In: Clark MJ (ed) Advances in periglacial geomorphology. Wiley, Chichester, pp 3–31
Thorn CE, Hall K (2002) Nivation and cryoplanation: the case for scrutiny and integration. Prog Phys Geogr 26:533–550
Thorn CE, Darmody RG, Campbell SW, Allen CE, Dixon JC (2007) Microvariability in the early stages of cobble weathering by microenvironment on a glacier foreland, Storbreen, Jotunheimen, Norway. Earth Surf Proc Land 32:2199–2211
Thorn CE, Darmody RG, Dixon JC (2011) Rethinking weathering and pedogenesis in alpine periglacial regions: some Scandinavian evidence. In Martini IP, French HM, Pérez Albert A (eds) Ice-marginal and periglacial processes and sediments, vol 354. Geological Society, London, Special Publication, pp 183–193
Tikkanen M (2005) Climate. In: Seppälä M (ed) The physical geography of Fennoscandia. Wiley-Blackwell, Chichester, pp 97–112
Tikkanen M, Heikkila R (1991) The influence of clear felling on temperature and vegetation in an esker area at Lammi, southern Finland. Fennia 169:1–24
Ulfstedt AC (1993) Solifluction in the Swedish mountains: distribution in relation to vegetation and snow cover. In: Frenzel B, Matthews JA, Gläser B (eds) Soliflucton and climatic variation in the Holocene. Gustav Fischer Verlag, Stuttgart, pp 217–223

Van Vliet-Lanoë B, Seppälä M (2002) Stratigraphy, age and formation of peaty earth hummocks (pounus), Finnish Lapland. Holocene 12:187–199

Van Vliet LB, Seppälä M, Käyhkö J (1993) Dune dynamics and cryoturbation features controlled by Holocene water level changes, Hietatievat, Finnish Lapland. Geol Mijnbouw 72:211–224

Vere DM, Matthews JA (1985) Rock glacier formation from a lateral moraine at Bukkeholsbreen, Jotunheimen, Norway: a sedimentological approach. Zeitschrift für Geomorphologie NF 28:397–415

Vasskog K, Nesje A, Støren EN, Waldmann N, Chapron E, Ariztegui D (2011) A Holocene record of snow-avalanche and flood activity reconstructed from a lacustrine sedimentary sequence at Oldevatnet, western Norway. Holocene 21:597–614

Vogt T (1918) Om recente og gamle strandlinjer I fast fjell. Norsk Geologiske Tidsskrift 4:107–127

Vorren KD (1979) Recent palsa datings, a brief survey. Nor Geogr Tidsskr 33:217–219

Vorren KD, Vorren B (1975) The problem of dating a palsa, Two attempts involving pollen diagrams, determination of moss subfossils, and C14-datings. Astarte 8:73–81

Vorren TO, Mangerud J, Blikra LH, Nesje A, Sveian H (2006) Landet trer fram. In: Ramberg IB, Bryhni I, Nøttvedt A (eds) (2006) Landet blir til: Norges geologi (Chapter 16, 532–555). Norsk Geologisk Forening (NGF): Trondheim. 608 pp

Walker MJC, Head MJ, Berkelhammer M, Björck S, Cheng H, Cwynar L, Fisher D, Gkinis V, Long A, Lowe JJ, Newnham RJ, Rasmussen SO, Weiss H (2018) Formal ratification of the subdivision of the Holocene Series/Epoch (Quaternary System/Period): two new Global Boundary Stratotype Sections and Points (GSSPs) and three new stages/subseries. Episodes 41:213–223

Washburn AL (1979) Geocryology: a survey of periglacial processes and environments. Arnold, London

Wilford DJ, Sakals ME, Innes JL, Sidle RC, Bergerud WA (2004) Recognition of debris flow, debris flood and flood hazard through watershed morphometrics. Landslides 1:61–66

Williams PJ (1957) Some investigations into solifluction features in Norway. Geogr J 23:42–58

Williams PJ (1961) Climatic factors controlling the distribution of certain frozen ground phenomena. Geogr Ann 43:339–347

Wilson P, Matthews JA, Mourne RW (2017) Relict blockstreams at Insteheia, Valldalen-Tafjorden, southern Norway: their nature and Schmidt-hammer exposure age. Permafrost Periglac Process 28:286–297

Wilson P, Linge H, Matthews JA, Mourne RW, Olsen J (2019) Comparative numerical surface exposure-age dating (^{10}Be and Schmidt hammer) of an early-Holocene rock avalanche at Alstadfjellet, Valldalen, southern Norway. Geogr Ann Ser (Phys Geogr) 101:293–309

Wilson P, Matthews JA, Mourne RW, Linge H, Olsen J (2020) Interpretation, age and significance of a relict paraglacial and periglacial boulder-dominated landform assemblage in Alnesdalen, Romsdalsalpane, southern Norway. Geomorphology 369: Article No. 107362 (16 p).

Winkler S, Matthews JA, Mourne RW, Wilson P (2016) Schmidt-hammer exposure ages from periglacial patterned ground (sorted circles) in Jotunheimen, Norway, and their interpretive problems. Geogr Ann Ser (Phys Geogr) 98:265–285

Winkler S, Matthews JA, Haselberger S, Hill JL, Mourne RW, Owen G, Wilson P (2020) Schmidt-hammer exposure-age dating (SHD) of sorted stripes on Juvflye, Jotunheimen (central southern Norway): morphodynamic and palaeoclimatic implications. Geomorphology 353: Article No. 107014 (19 p).

Winkler S, Donner A, Tintrup gen Suntrup A (2021) Periglacial landforms in Jotunheimen, central southern Norway, and their altitudinal distribution. In Beylich AA (ed) Landscapes and landforms of Norway. Berlin: Springer, pp 169-202

Worsley P (2008) Some observations on lake ice-push features, Grasvatn, northern Scandinavia. Nor Geogr Tidsskr 29:10–19

Worsley P, Harris C (1974) Evidence for Neoglacial solifluction at Okstindan, north Norway. Arctic 27:128–144

Zuidhoff FZ, Kolstrup E (2000) Changes in palsa distribution in relation to climate change in Laivadalen, northern Sweden, especially 1960–1997. Permafr Periglac Process 11:55–69